Geochemistry, Geophysics, Geosystems®

AGU ADVANCING EARTH AND SPACE SCIENCE

RESEARCH ARTICLE
10.1029/2021GC010045

Interaction Between Climate and Tectonics in the Northern Lesser Antilles Inferred From the Last Interglacial Shoreline on Barbuda Island

J. Weil-Accardo[1,2], N. Feuillet[2], B. Philibosian[2,3], A. Guihou[1], E. Jacques[2], G. Cabioch[4], A. Anglade[2,5], A.-S. Meriaux[6,7], and P. Deschamps[1]

[1]Aix Marseille University, CNRS, IRD, INRAE, CEREGE, Aix-en-Provence, France, [2]Paris University, Institut de physique du globe de Paris, CNRS, Paris, France, [3]Now at U.S. Geological Survey Earthquake Science Center, Moffett Field, Mountain View, CA, USA, [4]IRD, UMR OCEAN, Bondy, France, [5]Now at I3S, CNRS, Universite Cote d'Azur, Sophia Antipolis, Antibes, France, [6]School of Geography Politics and Sociology, Newcastle University, Newcastle upon Tyne, UK, [7]Now at Institut Terre Environnement de Strasbourg, UMR 7063 CNRS, Strasbourg University, Strasbourg Cedex, France

Key Points:

- Highest Last Interglacial sea level indicator on Barbuda island is found at 9 ± 1 m above present mean sea level
- We present the first U-Th ages from corals found in growth position within the Last Interglacial marine terrace on Barbuda
- Barbuda may record subduction-related uplift superimposed on effects of various non-tectonic processes

Supporting Information:

Supporting Information may be found in the online version of this article.

Correspondence to:

J. Weil-Accardo,
weil@cerege.fr

Citation:

Weil-Accardo, J., Feuillet, N., Philibosian, B., Guihou, A., Jacques, E., Cabioch, G., et al. (2022). Interaction between climate and tectonics in the northern Lesser Antilles inferred from the Last Interglacial shoreline on Barbuda island. *Geochemistry, Geophysics, Geosystems*, *23*, e2021GC010045. https://doi.org/10.1029/2021GC010045

Received 19 JUL 2021
Accepted 21 APR 2022

Abstract In the context of increasing evidence of plate interface coupling variability in subduction zones, there is a need to extend the short time window given by instrumental data and to gather data over multiple time and spatial scales. We hence investigated the long-term topography on Barbuda island, located in the northern part of the Lesser Antilles, west of the Caribbean subduction zone. Following pioneering work using a set of marine terraces on the eastern side of the island, we performed the first U-Th dating on 10 corals in growth position from the lowest terrace, for which the highest relative sea-level (RSL) indicator is found at 9 ± 1 m above the mean sea level. We find that this terrace corresponds to the Last Interglacial (LIG) (ages between 122.8 ± 0.3 ka and 128.1 ± 0.3 ka) and we estimate a paleo RSL of 7 ± 2 m above the current mean sea level. The present elevation of the LIG shoreline on Barbuda might imply tectonics as an additional mechanism to eustatic sea level, mantle dynamic topography and glacial isostatic adjustment. East-west morphological asymmetry of Barbuda and difference in LIG shoreline elevation between Barbuda and Antigua suggest a regional tectonic process. As with the proposed westward tilting from the forearc to the volcanic arc of the Guadeloupe archipelago, vertical deformation on Barbuda could be related to plate-scale subduction processes. Long-term uplift of Barbuda might be related to the accumulation of residual coseismic deformation not fully recovered by interseismic subsidence and the corresponding seismogenic segment would extend below the Moho.

1. Introduction

The Lesser Antilles island arc is located on the eastern border of the Caribbean plate (Figure 1a), where the North and South American plates are subducting below the overriding Caribbean plate at a convergence rate of about 2 cm/yr (DeMets et al., 2000). The historical seismicity catalog, beginning with the first European settlements, mentions only two ≈ Mw 8 likely megathrust earthquakes, occurring 4 years apart, in 1839 and 1843 offshore Martinique and Guadeloupe islands, respectively (Figure 1a) (Feuillard, 1985; Feuillet, Beauducel, & Tapponnier, 2011; Robson, 1964). With its low convergence rate, evidence of weak seismicity from the instrumental record, and lack of major earthquakes since the year 1900, the Lesser Antilles megathrust has often been considered as aseismic (Stein et al., 1982), corroborated by the low plate interface coupling derived from geodetic data (Manaker et al., 2008; Symithe et al., 2015; van Rijsingen et al., 2020). However, deformation patterns within the short time window provided by instrumental records might not be representative of the subduction interface behavior over longer timescales. Moreover, the spatial coverage of geodetic stations is sparse and instruments are often located far from the trench, where they may not be sensitive to small seismogenic fault patches.

Several lines of evidence, however, are not consistent with the conclusions of the short-term and sparse geodetic measurements. The existence of emergent and submerged marine terraces in the Guadeloupe archipelago (from the forearc to the arc) highlight a pattern of long-term vertical deformation, which has been interpreted to be linked to plate-scale subduction processes (Feuillet et al., 2004; Leclerc & Feuillet, 2019; Leclerc et al., 2014, 2015). In addition, long-term vertical deformations since the Neogene have been inferred from a sedimentary and tectonic analysis of the Karukera spur (submerged rise offshore the Guadeloupe archipelago) that might be related to a coupling change on the megathrust interface (De Min et al., 2015). Finally, coral microatolls in Martinique

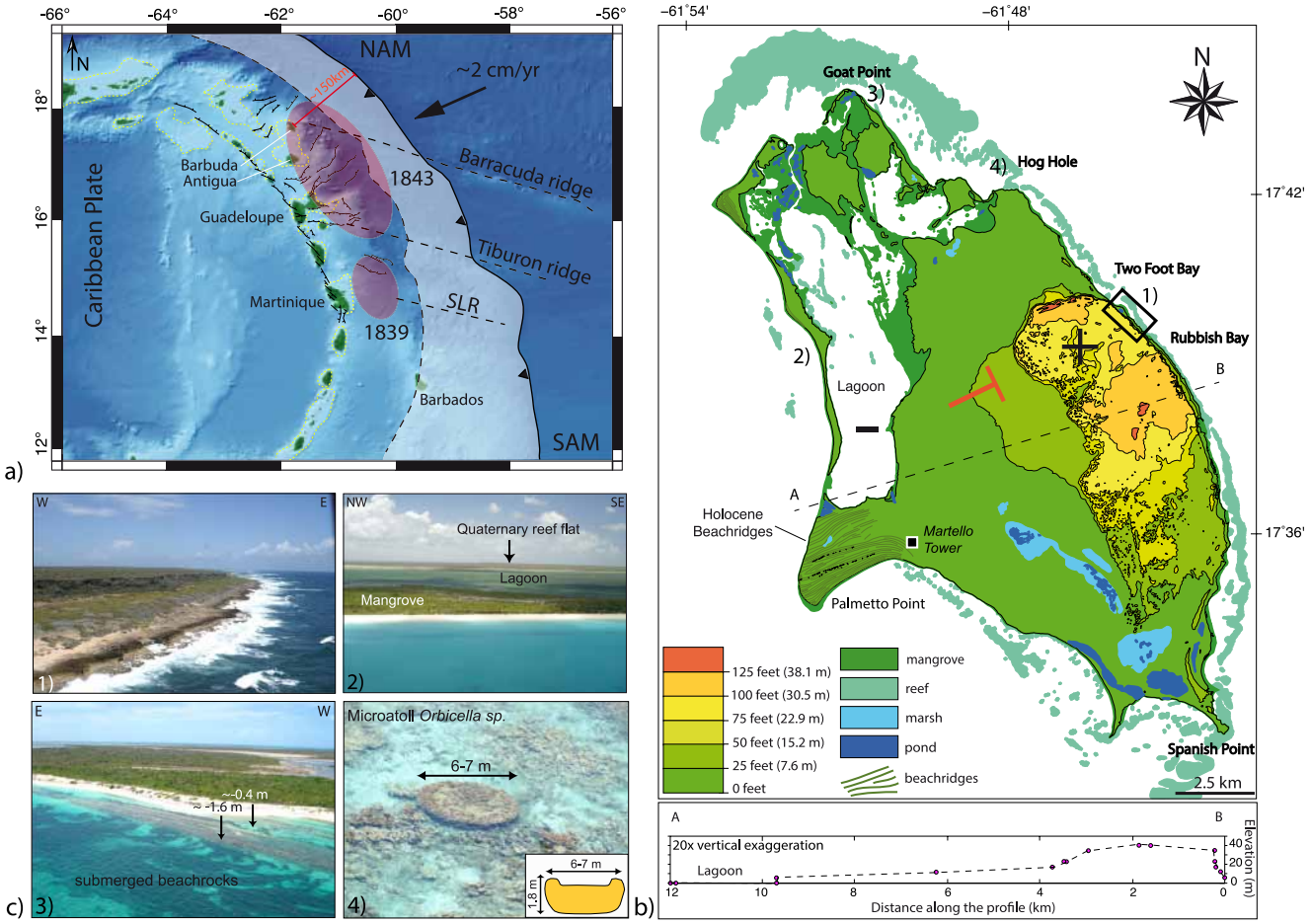

Figure 1. Geomorphology of Barbuda. (a) Geodynamic setting. Bathymetry and topography: SRTM30+ (horizontal resolution: 900 m). Active faults from Feuillet (2000), Feuillet et al. (2002, 2004), Feuillet, Beauducel, Jacques, et al. (2011), Leclerc (2014). Convergence rate and direction from DeMets et al. (2000). SLR: St. Lucia ridge. NAM and SAM: North American and South American Plates. Red ellipses: rupture areas for 1839 M8 and 1843 M8.5 earthquakes (Feuillet, Beauducel, Jacques, et al., 2011). Yellow dashed lines: submarine carbonate platforms. Black barbed line: accretionary prism frontal thrust. Dashed black line: primary negative gravity anomaly corresponding to the Lesser Antilles backstop (Bowin, 1976; Evain et al., 2013; Laigle et al., 2013; Westbrook et al., 1988). White shaded area: accretionary prism. (b) Topography and environments of Barbuda. Contours at 25-foot intervals derived from 1970 1:25,000-scale British Government Ministry of Overseas Development topographic map. Black rectangle highlights main study area between Two Foot Bay and Rubbish Bay. Red dip symbol indicates apparent southwestward tilting of the island (mainly based on island morphology). Elevation profile (with 20x vertical exaggeration) along line A-B is shown below the map with control points from the topographic map indicated by pink dots. Numbers (1–4) indicate locations of the pictures in part (c). (c) Photographs taken during a helicopter survey showing (1) terraces in study area on east coast, (2) lagoon and flat topography on west coast, (3) submerged beachrocks at Goat Point, and (4) large microatoll in Hog Hole.

provide evidence of interseismic subsidence of the island and one instance of coseismic subsidence related to the Mw 71,946 subduction earthquake (Weil-Accardo et al., 2016). Studies of coral microatolls in the Antilles and elsewhere have also revealed discrepancies between deformation patterns recorded over different time scales, likely related to variability of the megathrust seismic behavior (e.g., Meltzner et al., 2015; Philibosian et al., 2014; Philibosian et al., 2022; Weil-Accardo et al., 2020, 2016). Overall, these observations of vertical deformation along the Lesser Antilles arc over multiple time scales imply stronger long-term interplate coupling than inferred from geodetic data.

Furthermore, giant megathrust earthquakes that occurred in the past two decades in Indonesia and Japan provide new insights into subduction zone behavior and challenged the classic consensus that low seismicity, low convergence rate, or old subducting plate imply aseismic subduction (e.g., Ruff & Kanamori, 1980; Ruff & Kanamori, 1983). In fact, McCaffrey (2008) concluded that no subduction zone can be defined as aseismic and unable to generate large earthquakes based on those criteria.

Given the increasing evidence of coupling variability along subduction zones (e.g., Meltzner et al., 2015; Philibosian et al., 2014; Weil-Accardo et al., 2016, 2020), there is a need to extend the instrumental-time window of investigation and integrate multiple temporal and spatial scales to build a more accurate understanding of the megathrust seismic behavior.

In that regard, marine terraces are morphological evidence documenting past relative sea-level (RSL) changes which, corrected for the absolute sea-level change component, have often been used to establish the history of vertical deformation of coastal areas (e.g., Chappell, 1974). More particularly, and despite uncertainty on their paleo-depth, fossil coral reefs, which can be dated precisely with radiometric techniques, have been widely used to document past RSL changes (e.g., see compilation in Hibbert et al., 2016). The present study focuses on Barbuda island where a flight of emergent marine terraces has been previously described by Russell and McIntire (1966), Brasier and Mather (1975), Brasier and Donahue (1985). Barbuda, located in the northern Lesser Antilles, is one of the Outer Leeward Islands that form a limestone arc eastward of the volcanic islands of the inner arc. Located about 150 km west of the subduction deformation front, it is, along with La Désirade island and Barbados, one of the land masses closest to the deformation front and is thus a key area capable of having a geologic record of a stronger signal from megathrust behavior.

This paper presents results from fieldwork conducted on Barbuda between 2009 and 2013, which include more precise surveying of the terrace elevations and the first U-Th dating, in comparison to previous studies (detailed in the next section). After summarizing previous work conducted on Barbuda, we explain the methodology used for terrace mapping and U-Th dating of a fossil reef. We then present the results and discuss them in the context of the current understanding of RSL changes of various origin.

2. Previous Work on Barbuda Geology

Throughout the previous published works on Barbuda geology, there has been a debate about the age of the island. Some investigators have suggested a Pleistocene age, which implies uplift (Harris, 1965; Martin-Kaye, 1959; Russell & McIntire, 1966), possibly due to subduction of the Barracuda ridge (McCann & Sykes, 1984). Alternatively, Brasier and Mather (1975), Brasier and Donahue (1985) propose that Barbuda is tectonically stable and that its elevation mainly reflects sea-level oscillations since Mid-Miocene or Early Pliocene time.

The surface of Barbuda island is divided into two major geologic units, the "Highlands" and the "Lowlands" (Martin-Kaye, 1959; Russell & McIntire, 1966). The "Lowlands" are further separated into three units that were identified using aerial photographs and through stratigraphic and sedimentary field studies supplemented with microfacies and foraminifera assemblage analyses in thin section (Brasier & Donahue, 1985; Brasier & Mather, 1975). The most detailed relative chronology comprises four units, going from the lowest elevation (youngest) to the highest elevation (oldest): the "Palmetto point", "Codrington", "Beazer", and "Highlands" Formations (Brasier & Donahue, 1985; Brasier & Mather, 1975) (Figure S1 in Supporting Information S1).

The Palmetto Point Formation was estimated to be of Holocene age (Brasier & Donahue, 1985; Brasier & Mather, 1975). At Palmetto Point, on the central west coast of Barbuda, and in a few other places on the west coast, the formation is composed of a system of beach ridges prograding toward the sea (Russell & McIntire, 1966). ^{14}C dating of *Strombus* fragments from a lithified limestone ridge that might mark a paleoshoreline in the Palmetto point area confirmed a mid-to late Holocene age (Watters et al., 1992). The Codrington Formation is hypothesized to be related to the Last Interglacial (LIG) (Brasier & Donahue, 1985; Russell & McIntire, 1966). This formation is the product of a period of marine transgression to about 6 m above the present sea level which promoted reef building, followed by a marine regression with reef emergence, lagoon closing and beach ridge progradation (Brasier & Donahue, 1985). No U-Th dating was performed to confirm the LIG age. Russell and McIntire (1966) observed that the Codrington Formation is higher on the east coast than anywhere else on the island, and proposed that it might express tilting due to crustal deformation or be related to depositional topography during the LIG (similarly to modern reef distribution which is more developed on the east).

The Beazer Formation, assumed to be Early Pleistocene (Brasier & Donahue, 1985; Brasier & Mather, 1975) is observed up to 15 m elevation with a possible secondary level at about 10 m. The deposits are typical of a shallow marine environment. The western bays and fringing reefs around the rest of the island would have developed during that period (Brasier & Donahue, 1985).

The age of the Highlands Formation, which culminates at nearly 40 m elevation, is debated. Several authors proposed a Tertiary age, Middle Miocene to Early Pliocene (Andreieff et al., 1987; Brasier & Donahue, 1985; Brasier & Mather, 1975), that is compatible with the degree of alteration (no remaining aragonite, very low level of strontium) according to Wigley (1977) and supported by coralgal facies (rich in coral, coralline algae, and reefal aggregates) and foraminifera assemblages (Brasier & Donahue, 1985; Brasier & Mather, 1975; Wigley, 1977). Recent work of Cornee et al. (2021) using benthic foraminifera also suggests a late Miocene - early Pliocene age. In contrast, Martin-Kaye (1959), Russell and McIntire (1966) suggested a Pleistocene age (mainly based on evidence of a Late Pleistocene highstand elsewhere at regional and global scales). Thin section analysis of this older limestone, which appears superficially unfossiliferous, indicates a reefal environment (Wigley, 1977) with an original depth of deposition ranging between 20 and 100 m (Brasier & Donahue, 1985).

Between each of the formations, the sea level would have dropped, making the emergent formations subject to karstic erosion and alteration.

Among published works on Barbuda geology, apart from the Holocene, there is a lack of any numerical chronological data. Consequently, the chronology is mainly based on comparison with surrounding islands and paleontology (e.g., Brasier & Donahue, 1985; Brasier & Mather, 1975; Cornee et al., 2021). Also, surveying was not as accurate as today and there were no precise elevation measurements relative to mean sea level in any of these published works. In light of the technological progress in both surveying and dating, our reinvestigation of the island can significantly improve on these pioneering studies and provide better insight into the tectonic or glacio-eustatic nature of past RSL changes there. To resolve the chronology of formation and the surface processes involved, we surveyed the set of marine terraces across a small transect on the east coast of the island and performed U-Th dating on samples collected from the lowest Codrington Formation.

3. Methodology

3.1. Terrace Mapping and Survey

We used a 1970 1:25,000 topographic map from the British Government Ministry of Overseas Development as a base (Figure 1b), before adding field survey data to enhance it in our study area. We hence extracted contours every 25 feet from 0 to 125 feet (about 38 m) over the entire island (Figure 1b). A highest point is noted on the map at about 128 feet (≈39 m). This process provided a crude understanding of the geomorphology of Barbuda.

Our field survey of the terrace topographic profile (Figures 2g–2i) was done using a Total Station (TS) with high vertical precision (ranging between a few millimeters to ±0.2 m depending on distance of the surveyed point from the base station and on meteorological conditions, Rovere et al., 2016; Weil-Accardo et al., 2016). The measurements of RSL indicators along a transect perpendicular to the coastline (abrasion surfaces, notches, corals in growth position) are referenced to the observed sea level at the time of the survey. According to the Service hydrographique et océanographique de la Marine tide predictions in Saint-Martin and La Désirade in the Lesser Antilles, the sea level was increasing toward the high tide the days we surveyed the site (Figure S2 in Supporting Information S1). Therefore, our measured elevations could be slightly lower than the true elevations above mean sea level (MSL). However, since the tidal range in Barbuda is small, on average about 40–50 cm, an uncertainty of ±0.25 m was added to the survey elevations to account for the effects of tidal range. The overall vertical uncertainties of the surveyed elevations are estimated to be ±0.5 m relative to MSL.

A kinematic Global Positioning System (GPS) profile performed along the same survey path as the TS profile gives consistent measurements with TS data, while a few other GPS measurements outside the surveyed area helped us to better localize the 25-foot contour line from the 1:25,000-scale British Government Ministry of Overseas Development topographic map in the area investigated (Figure S3 in Supporting Information S1). Because the 25-foot contour line is observed about 1.5–2 m below the lower major notch we noted in the field (Figure 2c), it can be used to estimate the position of the terrace boundaries over longer distances.

3.2. Coral Sampling and U-Th Dating With MC-ICPMS

Looking for datable material within the terraces, we scouted for corals in growth position. The samples were chosen using the usual visual and audible criteria to distinguish between altered or preserved aragonite (e.g.,

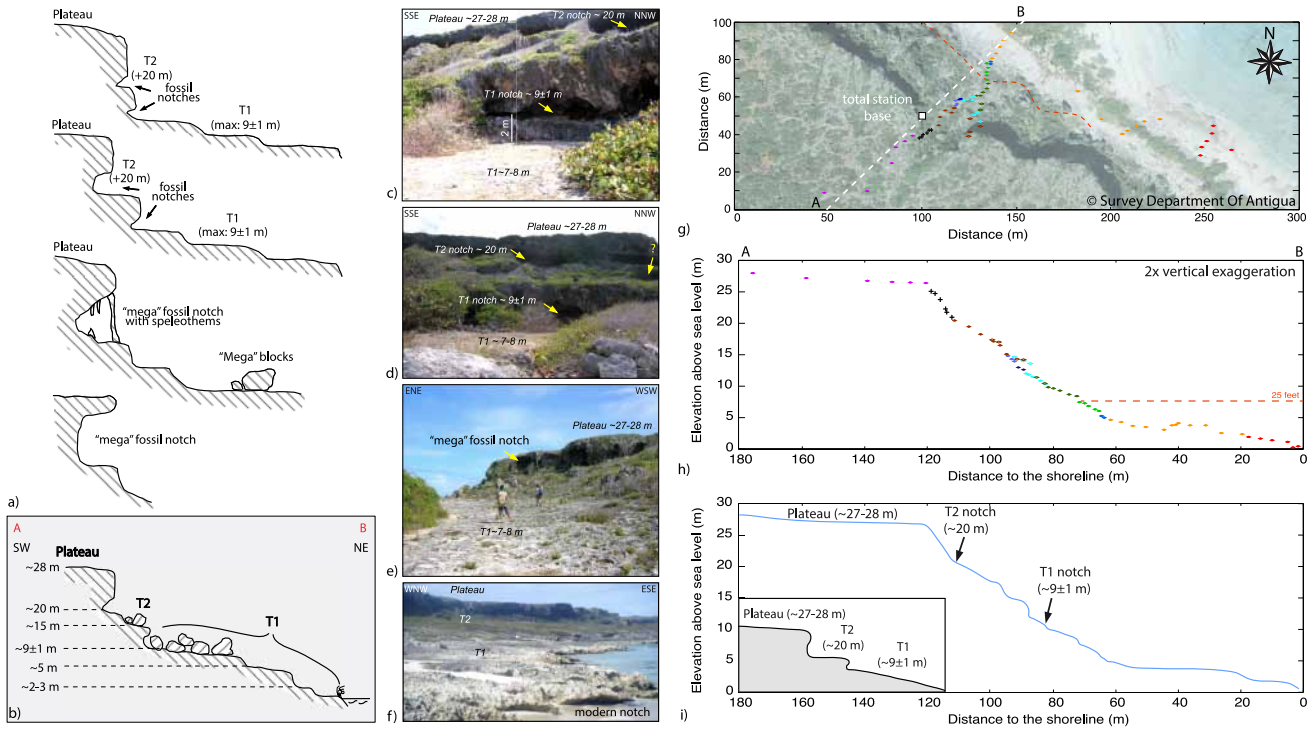

Figure 2. Terrace surveys. (a) Sketches illustrating the variety of terrace profiles along the coast. (b) Profile sketch that summarizes our observations. (c, d, and e) Photographs of the terraces annotated to mark major terrace levels and notches (yellow arrows). (f) Photograph showing small modern notch along with terraces T1, T2 and the plateau. (g) Map view of the Total Station (TS) survey on aerial image from the Survey Department of Antigua-Barbuda. White square: TS base. Diamond symbols with different colors indicate distinct surfaces identified in the field during the TS survey. Black crosses: eroded cliff. Dashed red lines indicate 25-foot contour line from the 1:25,000-scale British Government Ministry of Overseas Development topographic map. That contour is about 1.5–2 m below the lower notch (c) we observed, and we drew it on the elevation profile in panel (h) to project the location of the eroded notch along the TS profile surveyed. (h) Elevation profile of surveyed points projected along line A-B in part (g). Symbols as in panel (g). (i) Interpretation of the TS profile. Large arrows indicate the T1 and T2 paleo-notches. Inset in the lower left corner shows simplified averaged topography observed all along the investigated area with three main terraces.

Edwards et al., 2003). We thus favored samples that were lightweight and not shiny, with preserved internal roughness and that did not sound high-pitched when hit by the hammer.

Mineralogical analyses and U-Th dating were carried out at CEREGE. After visual examination with binocular microscope and prior to U-Th analysis, X-ray diffraction analyses were performed on all samples to identify any postmortem diagenetic alteration of their aragonite skeletons. Calcite content was estimated with the calibration equation obtained on the X'PERT PRO machine by Sepulcre et al. (2009). Only samples with less than 1% calcite were considered for U-Th dating. U-Th analyses were performed using a double ^{236}U-^{233}U-^{229}Th spike calibrated against an aliquot of the Harwell HU-1 uraninite standard originating from GEOTOP (see Deschamps et al., 2012, for details). U-Th ages were calculated using the half-lives provided by Cheng et al. (2013) for ^{230}Th (75,584 years) and ^{234}U (245,620 years). Details of the chemical procedure and analyses conducted on a MC-ICPMS NEPTUNE (following the procedure of Chiang et al., 2019) are given in Appendix A.

4. Results

4.1. Terrace Elevations

From the topographic map (Figure 1b), we observe that most of the topography is concentrated in the central eastern part of the island with a highest point that stands at 39 m of elevation, while the remaining low-lying parts of the island stand between 7 and 8 m and sea level, with development of shrubby maritime vegetation, marshes, and mangroves close to sea water (Figure 1b). The high-relief eastern coast contrasts with the large lagoon observed on the west and north sides of the island (Figures 1b and 1c) highlighting the east-west morphological asymmetry of Barbuda.

Table 1
U-Th Ages and Elevations Relative to Mean Sea Level of Corals From T1 in Two Foot Bay

Sample ID	Elevation (m)	^{238}U (ppb)	^{232}Th (ppt)	^{230}Th (ppt)	[^{234}U/^{238}U]	[^{230}Th/^{238}U]	[^{230}Th/^{232}Th]	Age (ka)	$\delta^{234}U_i$ (‰)
BARB-09-02	1.5 m	2888.4 (4.9)	282.5 (0.7)	35.83 (0.06)	1.106 (0.002)	0.759 (0.002)	23711 (69)	122.81 (0.33)	150.2 (1.1)
BARB-09-03	1.5 m	3206.9 (5.4)	115.5 (0.3)	40.60 (0.07)	1.104 (0.001)	0.775 (0.002)	65740 (210)	128.12 (0.34)	149.0 (1.0)
BARB-09-05	2.5 m	2591.6 (4.0)	214.9 (0.5)	32.09 (0.05)	1.104 (0.001)	0.757 (0.002)	27917 (84)	122.95 (0.30)	147.0 (1.0)
BARB-09-16	5 m	2960.0 (5.0)	575.7 (1.3)	37.04 (0.07)	1.102 (0.001)	0.766 (0.002)	12031 (35)	125.79 (0.33)	145.4 (1.0)
BARB-09-17	5 m	2505.2 (4.1)	168.1 (0.4)	31.05 (0.06)	1.103 (0.001)	0.758 (0.002)	34537 (108)	123.3 (0.31)	146.2 (0.9)
BTFB-13-01	2.5 m	2515.6 (3.9)	646.6 (1.6)	31.31 (0.05)	1.105 (0.001)	0.761 (0.002)	9056 (27)	123.87 (0.31)	148.9 (1.0)
BTFB-13-02	2.5 m	2794.0 (4.8)	74.7 (0.3)	34.73 (0.06)	1.103 (0.001)	0.760 (0.002)	86906 (338)	124.01 (0.32)	146.3 (1.0)
BTFB-13-03	2.5 m	2581.3 (4.2)	219.0 (0.6)	32.28 (0.06)	1.106 (0.001)	0.765 (0.002)	27568 (88)	124.70 (0.32)	150.9 (0.9)
BTFB-13-07	5 m	2588.9 (4.0)	448.4 (1.0)	32.28 (0.06)	1.103 (0.001)	0.763 (0.002)	13461 (39)	124.78 (0.30)	146.1 (0.9)
BTFB-13-08	<1 m	2708.4 (4.5)	369.0 (0.9)	33.94 (0.06)	1.105 (0.001)	0.767 (0.002)	17200 (66)	125.33 (0.32)	150.1 (0.9)

Note. Values in parentheses are $\pm 2\sigma$ absolute uncertainties. Square brackets denote activity ratios. Decay constants are 9.1705×10^{-6} yr^{-1} for ^{230}Th, 2.8221×10^{-6} yr^{-1} for ^{234}U (Cheng et al., 2013), and 1.55125×10^{-10} yr^{-1} for ^{238}U (Jaffey et al., 1971). Ages are reported relative to the year of analysis, 2020, and do not include uncertainties associated with decay constants.

On the timescale of the Holocene, Russell and McIntire (1966), Brasier and Donahue (1985) noted a well-developed prograding beach ridge system on the leeward western coast, contrasting with the windward eastern coast. Modern fringing and barrier reefs are, however, well-developed on the east and less so on the west.

Our field work allowed us to refine the preliminary mapping shown in Figure 1b. Between Two Foot Bay and Rubbish Bay, both sites located on the east coast of the island (Figure 1b), we studied a set of marine terraces that displays a classic staircase morphology (Figure 1c, picture 1 and Figures 2a–2e). These horizontal to gently seaward-sloping surfaces are flanked by slope-breaks or marked by paleo-notches along the landward edge. Indeed, two major paleo-notches about 10 m apart in elevation, often associated with caves (Figures 2c–2e) are persistent throughout the area. Near Two Foot Bay, we measured the topographic profile across 10 distinct surfaces distinguishable in the field (point colors in Figures 2g–2h) that range from 2–3 m to 27–28 m of elevation (Figure 2h). However, the major paleo-notches were less pronounced along the TS profile, so their elevations still have larger vertical uncertainty (±1 m). Based on field observations throughout the study area and the topographic survey, we estimate that these two major paleo-notches stand at elevations of about 9 ± 1 and 20 ± 1 m (Figures 2g–2i). Southward from Two Foot Bay, the number of apparent levels decreases, probably hidden by the vegetation, and only the paleo-notches remain identifiable. The maximum elevations of the two main levels that we interpret as wave-cut or reef terraces are at 9 ± 1 m (T1, Codrington unit) and 20 ± 1 m (T2), while the top of the plateau is found at 28 ± 1 m (Plateau). The other smaller meter-scale steps, less well preserved, are interpreted as secondary features.

The terrace T1 displays the widest horizontal surface, about 90 m, on the TS profile while terrace T2 is narrower, with a width of about 30 m (Figures 2g–2i). Large boulders that we assume fell from T2, above the paleo-notch, are found on T1 (Figures 2a and 2b, and S5 in Supporting Information S1).

4.2. Coral Sampling of the Codrington Formation

Most corals in growth position were found between sea level and 5 m (Table 1) and are interpreted to be a part of the Codrington Formation. The T1 terrace is thus the only level at the site where we found preserved corals. We collected 14 corals, mainly of genus *Pseudodiploria*, from two limited sections of T1, due to lateral variation with alternation of sandy facies and reefal facies (Figure 3a). Precision of elevation measurements of the samples at the time of their collection in 2009 was limited. Projection of the samples' GPS location (Figure 3a) on the TS survey profile (Figures 2e, 2g, and 3), done in 2013, provided better elevation estimates. Sample elevations range between less than 1 m and at least 5 m above mean sea level (Table 1, Figure 3). Other non-sampled corals were observed at elevations of 5 m and even higher, in altered areas that precludes any dating (Figure S4 in Supporting Information S1).

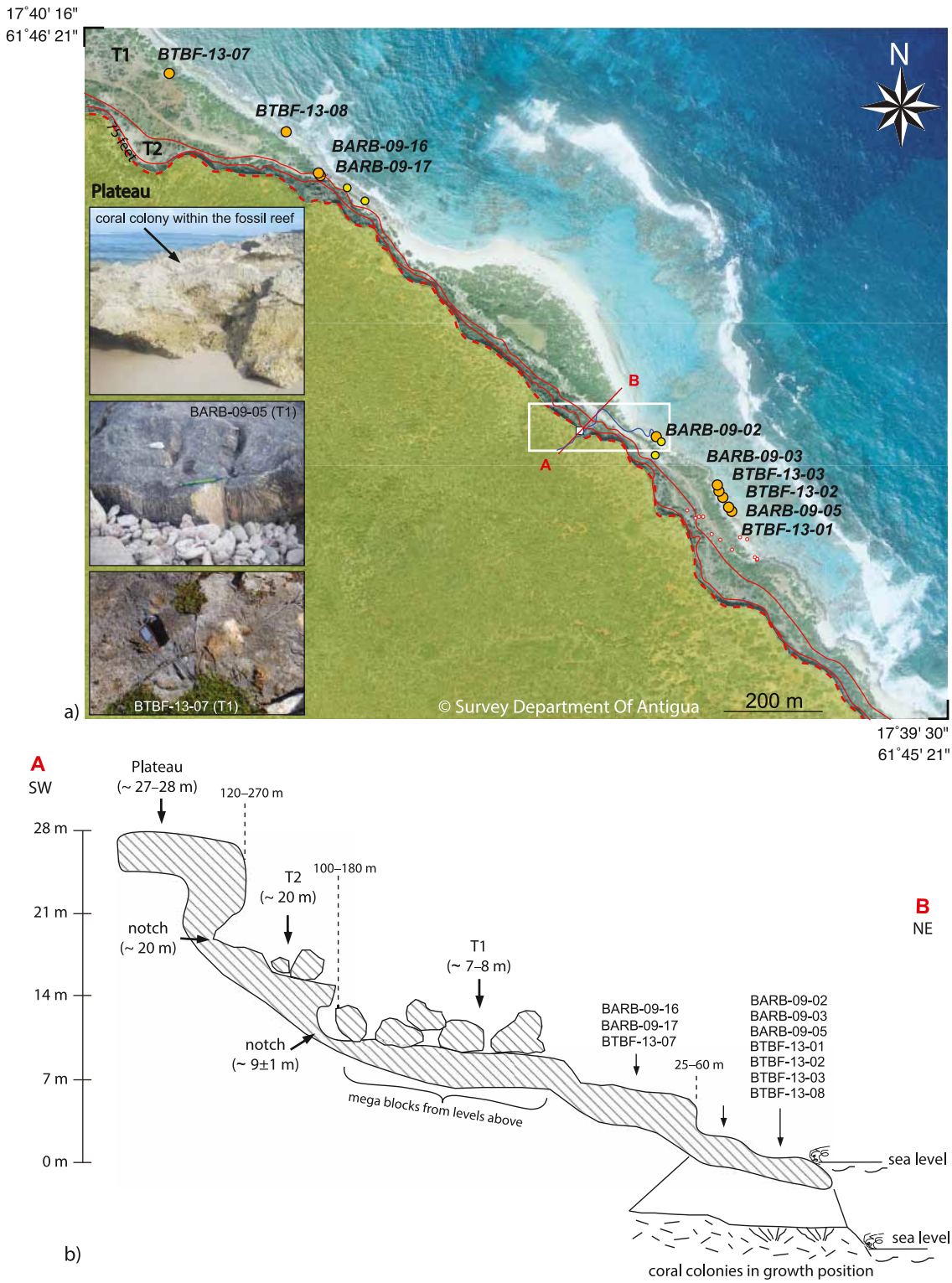

Figure 3.

As previously reported by Brasier and Donahue (1985), only altered coral rubble could be found in the Beazer Formation. Our scouting at the top of the plateau revealed a weathered surface with red soils that might be indicative of intense limestone alteration (Charter, 1937) or of external origin (African dust is a plausible source as it

has been proved to be a significant contributor to soils in Barbados, Florida, and the Bahamas, Muhs et al., 2007). No trace of datable corals was found on the plateau at the top of the Highlands Formation, as noted by previous authors.

4.3. U-Th Dating of the Codrington Formation

Among the 14 samples collected, 10 were 100% aragonite or contained less than 1% calcite. These 10 samples, therefore, were very suitable for dating with the uranium-thorium disequilibrium method. The ages fall between 122.8 ± 0.3 ka and 128.1 ± 0.3 ka (Table 1). We note that $^{230}Th/^{232}Th$ activity ratios of the samples are high (Table 1) implying low ^{232}Th concentrations and hence little evidence of any inherited ^{230}Th, indicating that any correction for detrital thorium would be negligible compared to other sources of age uncertainty (Edwards et al., 2003). The back-calculated initial $\delta^{234}U_i$ range between 145.4 ± 1.0‰ and 150.9 ± 0.9‰, with an average of 148.0 ± 3.8‰ (2SD) with very little dispersion around this value (Table 1). The initial $\delta^{234}U$ of this data set appears very homogeneous in comparison with data obtained for the Last Interglacial in other reefal outcrops (see compilation in Hibbert et al., 2016). This value is slightly higher than the value reported by Andersen et al. (2010) for the modern, open ocean seawater (i.e., 144.9 ± 0.4‰ when corrected for analytical biases, see Chutcharavan et al., 2018) and the value for modern coral (145.0 ± 1.5‰ Chutcharavan et al., 2018). However, it remains consistent with the range proposed by Hibbert et al. (2016) for interglacial corals (147 ± 5‰). In the present case, this slight departure from the modern, open ocean $\delta^{234}U$ signature cannot be considered as evidence of open-system behavior or post-depositional diagenesis. There are now several lines of evidence that the $^{234}U/^{238}U$ isotopic composition of the global ocean has varied at the glacial/interglacial scale on the order of at least a few ‰ (Chen et al., 2016; Chutcharavan et al., 2018). The $\delta^{234}U$ of seawater during the LIG is still not well constrained. As all our samples are pristine according to the most rigorous mineralogical criteria and have mutually agreeing initial uranium ratios, which likely precludes any open-system behavior, we conclude that our U-Th age results are accurate, and indicate that the development of the T1 terrace is associated with the LIG (and that its development in Barbuda falls in the middle of the 115–130 ka range of the Last Interglacial stage).

4.4. Relative Sea-Level Estimate of the Codrington Formation

In the area investigated, there are two main types of RSL recorders within the Codrington Formation: a fossil reef with corals in growth position and a paleo-notch that often forms a cave.

It is well known that most coral species are "depth-generalists" and can thus be found over wide vertical ranges down to 40 m depth (Carpenter et al., 2008; Veron, 1995). Given this large uncertainty on the paleowater depth of fossil corals, authors often implicitly assume that fossil corals were growing on a reef flat at depths of 3 m or less (Blanchon, 2011). While they are very useful for precisely constraining the timing of a paleo-sea level, their large indicative range limits their utility for estimating the precise elevation of paleo-sea level.

Conversely, sedimentary deposits and notches, while less easily datable, are generally considered to be more precise sea-level indicators that also respond more quickly to RSL changes. They are therefore able to record brief sea-level changes, unlike corals which are limited by their longer response time to sea-level changes (Hearty et al., 2007).

Following the methodology of Rovere et al. (2016) to calculate the paleo-RSL from the elevation of sea-level indicators, we attempt to estimate elevation of modern analogs for the two RSL indicators (Figure 4).

Barbuda is in a microtidal regime, with a total tidal amplitude of about 0.5 m and annual lowest tide about 0.23 m below MSL (according to SPOTL tide model, Agnew, 2012). Microatolls, which are massive corals living in the intertidal zone with upward growth limited by the annual lowest tide, are the highest corals in a modern reef. In

Figure 3. Locations of the U-Th coral samples. (a) Background: aerial image from the Survey Department of Antigua-Barbuda. Geographic coordinates are given for the upper left and the lower right corners of the image. Dashed red line indicates 75-foot contour that corresponds to the edge of the Plateau. 25-foot and 50-foot contour lines are also indicated with light red lines and in Figure S3 in Supporting Information S1. 25-foot contour line is near the T1/T2 boundary (about 1.5–2 m below the fossil notch observed at about 9 ± 1 m, Figure 1c). Orange dots indicate locations of dated coral samples. Yellow dots indicate locations of coral sampled but not dated due to their excessive calcite content. White rectangle outlines the survey area (Figure 2e); Total Station (TS) location, survey path (blue line), and profile line are also marked. Small red circles: kinematic Global Positioning System points taken outside the TS profile (Figure S3 in Supporting Information S1). Photographs of a few representative coral samples are shown on the left. (b) Terrace sketch with locations of the dated coral samples. Distances inland of steps between surfaces are indicated with vertical dashed black lines.

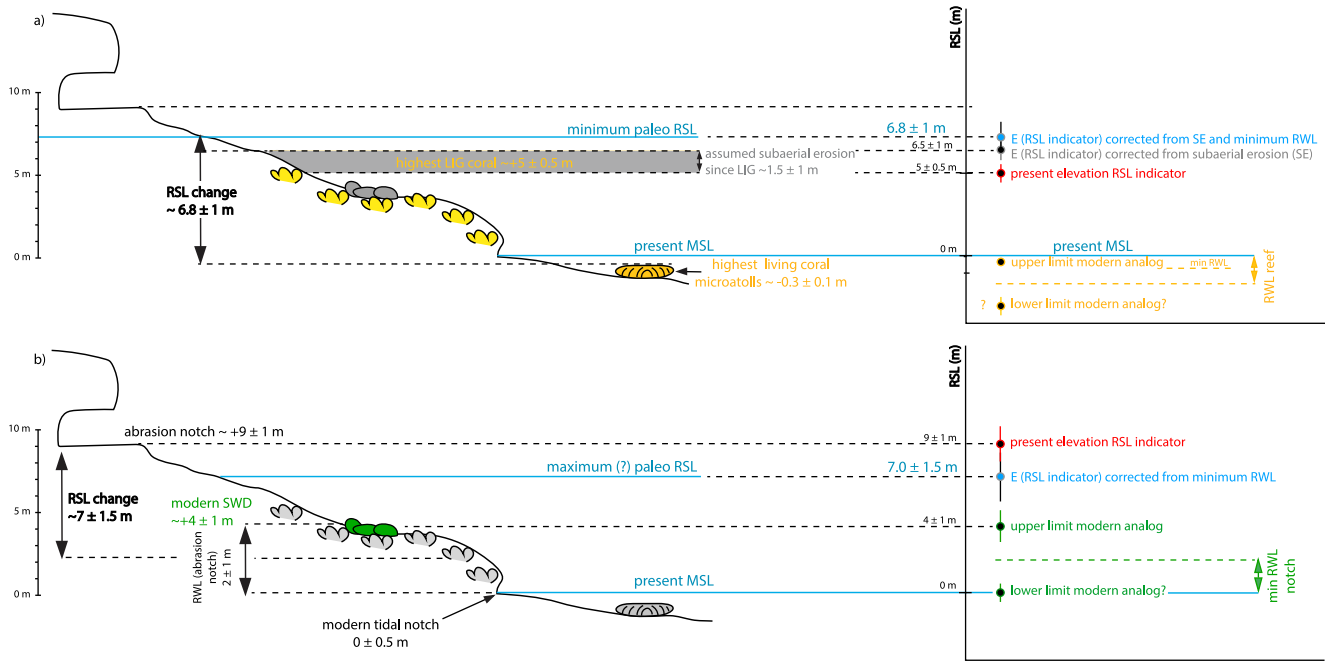

Figure 4. Schematic illustration of our calculations of the paleo Last Interglacial relative sea-level (RSL) change (following the methodology of Rovere et al., 2016) using the two paleo-RSL indicators: (a) the highest fossil corals and (b) the paleo abrasion notch. SWD: Storm wash deposits. RWL: Reference water level.

Hog Hole (location 4 in Figure 1b), Philibosian et al. (2022) measured their living upper surfaces at elevations ranging between 2 and 16 cm below the annual lowest tide, corresponding to depths of 25–39 cm below MSL, which we express as −0.3 ± 0.1 m relative to MSL (Figure 4a). Subaerial erosion might have planed off the fossil reef and lowered its elevation. Such erosion is difficult to estimate and prior studies give a large range of rates on reef limestone (between 0.011 and 0.75 m/ka, e.g., Opdyke et al., 1984; Paulay & McEdward, 1990; Spencer, 1985; Trudgill, 1979; Viles & Trudgill, 1984). At the low end of this range, subaerial erosion could have removed about 1.5 m since the LIG, while the rate at the high end would imply more than 90 m of reef removed, which is clearly implausible. Although the corals sampled and dated were found in place and not planed off, the higher part of the reef might have been eroded away. Using the lower published value for rate of limestone subaerial erosion, we thus assume that 1.5 ± 1 m of the top of the fossil reef might have been removed by erosion since the LIG. To estimate the paleo-RSL from the fossil reef, we corrected the RSL indicator elevation (highest dated fossil coral found in growth position at +5 ± 0.5 m relative to MSL) for subaerial erosion and the elevation of the highest modern corals. We thus get a final paleo-RSL of 6.8 ± 1 m above MSL from the fossil reef (Figure 4a). This estimate is a minimum since we do not know if the corals we observed in the fossil reef were microatolls and thus as close to sea level as modern living microatolls. Also, we used the lowest published rate for estimating the subaerial erosion, which might also lower the paleo-RSL estimate. Based on optimal depth of *Pseudodiploria* corals (genus is usually found between 1 and 3 m of the surface, e.g., Hibbert et al., 2016), we can estimate a probable paleo-sea level of 7 ± 1 m (ranging between 6 and 8 m for the highest corals sampled at 5 m of elevation), in agreement with our previous estimate.

Compared to the modern tidal notch which is rather subtle (Figure 2f) due to the small tidal range, the paleo-notch observed at about 9 ± 1 m above MSL spans a broader height (few meters, Figure 2c) and is interpreted to be an abrasion notch or a subaerial cave as described in Rovere et al. (2016). Its indicative range is higher than for a tidal notch with an upper limit given by the maximum elevation reached by extreme storm waves on the beach and a lower limit given by the breaking depth (Rovere et al., 2016). To find a modern analog, we noted a few areas of coral rubble amid the vegetation on the fossil reef, which we infer to have been brought there during storm events and for which we estimated a maximum elevation of 4 ± 1 m above MSL (Figure S6 in Supporting Information S1). However, the exact position of the breaking depth, below MSL, is more difficult to estimate, and we thus consider the present tidal notch at 0 ± 0.5 m of elevation relative to MSL as the lower limit of the modern abrasion notch. We thus calculate a reference water level (RWL) for the abrasion notch of 2 ± 1 m, which

is likely a minimum value (Figure 4b). By subtracting the RWL from the elevation of the paleo abrasion notch, we estimate a paleo-RSL at 7 ± 1.5 m of elevation above MSL (Figure 4b). This estimate, which is similar to the value inferred from the fossil reef, should be considered as a maximum since the RWL might be higher than what we calculated.

In summary, considering all the data, we obtain a mean paleo-RSL of 7 ± 2 m above modern MSL for the LIG sea level in Barbuda.

Change in tidal range would impact the indicative meaning of a sea-level indicator and hence the corresponding paleo-RSL estimate. In the Caribbean, the paleotidal range remained relatively constant through the Holocene according to modeling by (Khan et al., 2017). Earlier, in Pleistocene time, there have been very few sea-level studies that considered that parameter. On Bonaire island, the comparison of geometrical properties between a modern notch and a paleo notch formed during LIG suggested an insignificant change in tidal range (Lorscheid et al., 2017). Tidal modeling in the southern Caribbean (with modern and paleo bathymetry as the main inputs of the model since tidal amplitude would be primarily sensitive to coastal geometry over the Quaternary according to Hill, 2016) confirmed a negligible change in tidal range for Bonaire island (Lorscheid et al., 2017). However, change in tidal range becomes significant southward for the large shelf of the Gulf of Venezuela (with a paleo tidal amplitude about 15% larger than the modern tidal range, increasing in the very shallow part of the Gulf of Venezuela, Lorscheid et al., 2017). Barbuda is part of the Antigua-Barbuda shelf and might, similarly to the shallow part of the Gulf of Venezuela, have recorded a higher tidal range during the LIG. Nevertheless, 15% of the modern microtidal range remains negligible compared to the uncertainty of our final paleo-RSL estimate.

5. Discussion

5.1. Eustatic Sea Level

The existence of meter-scale sea-level fluctuations within the LIG highstand, that would imply periods of melting and regrowth of ice caps, is still debated (e.g., Barlow et al., 2018; Blanchon et al., 2009; Dutton, Carlson, et al., 2015; Hearty et al., 2007; R. E. Kopp et al., 2013; O Leary et al., 2013; Polyak et al., 2018; Rohling et al., 2019; Thompson & Goldstein, 2005). Direct evidence for such SL oscillations within the LIG mainly consists of high fossil notches observed in the Bahamas and Bermuda (at higher elevation than fossil corals) that are interpreted to reflect short-term SL stillstands (Hearty et al., 2007). However, recent work of Muhs et al. (2020) that revised elevations and dating of LIG sea-level markers in the Bahamas and Bermuda to test glacial isostatic adjustment (GIA) modeling supports a unique LIG highstand. In addition, in south Florida, the study of Muhs et al. (2011) focused on fossil reef complex and oolitic marine sediment formation does not support sea-level fluctuations within LIG. The stratigraphic analysis and U-Th dating of Blanchon et al. (2009) in the northeast of the Yucatan Peninsula, where the authors identified two reef tracts separated by about 3 m with a younger age (around 120 ka) for the upper level at 6 m, is rare coral-based evidence for a sea-level increase at the end of the marine isotope stage (MIS) 5e (although some samples from the lower reef might express open-system behavior).

Despite our field observations of morphological steps within the T1 reef terrace, with three corals sampled from a slightly higher level than the remaining dated samples (Figure 3b), our set of ages does not suggest any trend between age and elevation (Table 1). Rather, we have several ages around the same elevation that might reflect the natural reef heterogeneity and suggest a prograding reef growing below a stable sea level (Hibbert et al., 2016). However, the dated samples are restricted to small sections of T1 and most of the samples are located close to the present shoreline.

Notches are difficult to date and we might be tempted to interpret the abrasion notch at +9 ± 1 m above MSL as evidence of a brief RSL highstand higher than the stillstand recorded by the fossil reef at 5 ± 0.5 m above MSL (as suggested for notches in Bermuda and the Bahamas by Hearty et al., 2007). However, the depth of a notch into the cliff is related to rate, duration, and intensity of erosion (Trenhaile, 2015). Since the abrasion notch surveyed is deep and often associated with caves, it more likely formed during a marine stillstand. Moreover, our calculations of paleo-RSL during the LIG using the fossil reef and the paleo-notch are in good agreement with each other, which suggests that the two RSL indicators represent the same LIG highstand.

The LIG was a slightly warmer period than today, during which global mean sea level (GMSL) was higher as highlighted by most LIG sea-level benchmarks identified over the Earth's surface (e.g., R. E. Kopp et al., 2009). Through statistical approaches (e.g., R. E. Kopp et al., 2009) and modeling (e.g., Dutton & Lambeck, 2012) (using global database of LIG RSL indicators corrected for processes that might cause departure of local sea level from global sea level), it is now accepted that the maximum elevation attained by GMSL during the LIG was 6–9 m above the pre-industrial (Dutton & Lambeck, 2012; Dutton, Webster, et al., 2015; R. E. Kopp et al., 2009).

Although our mean paleo-RSL estimate of 7 ± 2 m falls within the 6–9 m range, it is well known that present elevations of LIG shorelines also reflect post-depositional vertical movement. Those vertical movements can be due to tectonics in areas close to active tectonic margins, or due to GIA that causes departures from eustasy close to former ice sheets, as well as in equatorial areas (Mitrovica & Milne, 2002). Moreover, Austermann et al. (2017) recently pointed out that mantle dynamic topography (DT), vertical crustal motion driven by mantle flow, may have caused vertical surface deformation of several meters since the LIG. There are thus several sources to consider when interpreting the present elevation of LIG markers in Barbuda. Comparison between elevations of LIG markers in surrounding areas is helpful to reveal possible vertical movements.

5.2. Comparison With Surrounding Areas

5.2.1. Comparison With Surrounding Tectonically Stable Areas

In surrounding tectonically stable coastlines, emergent coral reefs dated to the LIG were found at maximum elevation of 6 m above MSL in the northeast Yucatan Peninsula (Blanchon et al., 2009), 5.3 m above MSL in south Florida (Muhs et al., 2011) and at about 3 and 3.8 m above MSL in Bermuda and the Bahamas (with possible contribution of long-term subsidence for the Bahamas) (Muhs et al., 2020) (Figure S7 in Supporting Information S1).

Other RSL indicators dated to the LIG that usually form closer to sea level than coral reefs reach higher elevation. Beach ridge sediments on New Providence island in the Bahamas are found at elevations ranging between 5 and 10 m above MSL (Muhs et al., 2020), while a notch is found at 7 m above MSL on the Square Rock of Exuma Cays in the Bahamas (Hearty et al., 2007) (Figure S7 in Supporting Information S1). In south Florida, oolitic marine sediments are found at about 7 m above MSL (Muhs et al., 2011) (Figure S7 in Supporting Information S1). On Bermuda, where precise RSL indicators are less abundant (Muhs et al., 2020), no RSL indicators are found above 7.4 m (Muhs et al., 2020) (Figure S7 in Supporting Information S1).

Barbudan corals, at 5 ± 0.5 m above MSL, are found at similar elevation or higher than reefs of the same age in tectonically stable zones of the Caribbean (Figure S7 in Supporting Information S1). In addition, the paleo-notch at 9 ± 1 m above MSL, is higher than any other LIG RSL indicators studied in south Florida or in Bermuda (Muhs et al., 2020) (Figure S7 in Supporting Information S1) and higher than other notches in the Bahamas (Hearty et al., 2007) (Figure S7 in Supporting Information S1). This suggests that LIG markers have been uplifted in Barbuda. Moreover, no LIG RSL indicator is found at comparable altitude on the western side of the island where the main morphological feature is a lagoon filled by several meters of sediments (Bain et al., 2010; Biguenet et al., 2020). This indicates that the RSL markers of the LIG underwent vertical deformation after their deposition, as previously suggested by Russell and McIntire (1966).

5.2.2. Comparison Within the Lesser Antilles Arc

Regarding other islands of the Lesser Antilles, an interesting comparison can be made with the Guadeloupe archipelago. Similarly to the observation of the Barbuda LIG terrace being highest on the east coast (Russell & McIntire, 1966), the LIG terrace elevation varies throughout the Guadeloupe archipelago. On La Désirade island, the inner edge of the LIG terrace stands at 10 m (Battistini et al., 1986; Feuillet et al., 2004; Lardeaux et al., 2013; Léticée et al., 2019) and dated corals within the LIG terrace are found at elevations ranging between 2.5 and 5 m (Battistini et al., 1986; Feuillet et al., 2004; Léticée et al., 2019). In Grande-Terre, the LIG terrace stands at 5–6 m in the east (Léticée et al., 2019) and at 3–5 m in the north (Battistini et al., 1986); and in Marie-Galante the LIG terrace is found at 10 m elevation on the east and 2 m on the west (Battistini et al., 1986; Feuillet et al., 2004).

We hence note that LIG RSL indicators found in Barbuda, on La Désirade and on Marie-Galante stand at more or less similar elevations along the windward coast of the islands.

On Antigua, where we did a preliminary survey in 2009, we never observed indicators of a paleo-sea level (reef or notches) at elevations comparable to those on Barbuda along the windward coast. In addition, we can observe that Antigua island has a very different morphology than Barbuda characterized by embayed coastline (Figure S8a in Supporting Information S1) and smooth relief. Such a morphology is certainly a result of the long geological history of the island (e.g., Donovan et al., 2014), but may also indicate that the coasts are presently subsiding as observed elsewhere along the arc in Guadeloupe (Leclerc & Feuillet, 2019; Leclerc et al., 2014) or in Martinique (Leclerc et al., 2015). Contrasts in coastal morphology have also been inferred to indicate tectonic regional movement in other areas such as in the Ryukyus arc (with the islands of Kikai vs. Amami, Konishi et al., 1970) or the Gulf of Corinth (Armijo et al., 1996).

Between Willoughby and Mamora Bays, along the southeast coast (Figure S8 in Supporting Information S1), we identified a marine terrace 2 m above MSL made of indurated sand with no corals in growth position. This terrace was previously described by Multer et al. (1986) as a "skeletal sandy limestone" standing at an elevation of about 2 m. ^{14}C dating of one sample collected on this terrace indicated a late Holocene age. The very young age inferred from one sample was however taken with caution by Multer et al. (1986), who considered it as a minimum age and did not exclude the possibility that he might have missed older materials within the unit not suitable for radiocarbon dating. Indeed, this age is surprising considering that this terrace is strongly weathered and karstified (Figure S8b in Supporting Information S1) and resembles to marine terraces dated to the LIG in Guadeloupe and in Barbuda. Holocene reefs in Japan for example, are usually very well preserved (e.g., of Kikai island, Webster et al., 1998). Moreover, to our knowledge there are no markers of a late Holocene highstand on other islands of the Lesser Antilles comparable to those observed in other archipelagos in the Pacific ocean (e.g., ubiquitous platforms in the Ryukyus dated to mid to late-Holocene, Koba et al., 1982; Pirazzoli & Koba, 1989). Unless it was formed by a local uplift, this level is more likely older than Holocene. As its altitude is comparable to other terraces formed during the LIG in Guadeloupe, this marine terrace might have been also formed during the LIG.

In the following, we discuss the causal mechanisms that might be responsible for variation in elevation of LIG shoreline after its deposition in Barbuda.

5.3. Broad Scale Deformation Mechanisms

5.3.1. Mantle Dynamic Topography

Although DT is particularly relevant for million-year timescales (Rowley et al., 2013) it may also play a role in Quaternary RSL trends (Austermann et al., 2017; Rovere et al., 2014).

Along convergent plate boundaries, the spatial extent of the DT signal would be related to the subduction angle; the flatter the subduction, the broader the extent of the DT signal (a subduction angle of 25° would produce a signal over more than 1000 km of distance, Dávila & Lithgow-Bertelloni, 2013; Mitrovica et al., 1989). In the Caribbean, the seismicity that outlines the geometry of the interface highlights a dip that increases westward from 8° below the accretionary wedge, 14°–16° between 15 and 50 km of depth and higher than 35° beyond 50 km (Bie et al., 2020; H. Kopp et al., 2011; Ruiz et al., 2013). Variations in elevation of LIG markers that decreases westward within Barbuda (Russell & McIntire, 1966) and that might stand at 2 m along the southeast coast of Antigua would imply that the LIG shoreline is deformed over a spatial scale of a few tens of kilometers (25–50 km), which is likely too small to be ascribed to large scale DT. While DT generally acts on long wavelengths (several hundreds of km) (Dávila & Lithgow-Bertelloni, 2013; Mitrovica et al., 1989), there is evidence of DT signals on shorter spatial scales. Regarding a local DT signal, high-resolution tomographic imaging in the Lesser Antilles is restricted to the central Antilles (Guadeloupe to Martinique) and to the upper 30 km of depth (Evain et al., 2013; H. Kopp et al., 2011). Since the Caribbean crust is about that thick (e.g., H. Kopp et al., 2011), we are hence limited to the crustal structure of the Lesser Antilles arc and do not have access to the mantle structure. At larger scale, global tomography models are used for identifying regional anomalies in the upper mantle (e.g., Schaeffer & Lebedev, 2013) and are hence not detailed enough for our purposes. Seismic tomography at a resolution better than the island scale would help to characterize local mantle anomalies in the Lesser Antilles arc that differ from the regional DT signal related to the subduction (e.g., imaging of the subducting plate).

Despite the lack of accuracy at regional scale, the global-scale numerical modeling of Austermann et al. (2017) highlights that DT might have generated meter-scale RSL changes in Barbuda and uplifted the LIG terrace. Their model predicts 4 ± 4 m (1σ) of change in LIG elevation for the Lesser Antilles arc and 2 ± 2.5 m (1σ) in Barbuda.

DT impact on LIG shorelines of the Bahamas, south Florida, and Bermuda would trend in the same direction as in Barbuda, uplifting the LIG shorelines with a similar amplitude in the Bahamas and south Florida, and a stronger amplitude for Bermuda (Austermann et al., 2017) (Figure S7 in Supporting Information S1). Across the Yucatan peninsula, DT seems to vary with strong positive to slightly negative signal (Austermann et al., 2017).

5.3.2. Glacial Isostatic Adjustment

GIA impact on RSL is well understood (in terms of pattern expected) and well documented, especially for the last glacial cycle (Lambeck & Chappell, 2001). We know for example, that sites like the Caribbean, located in the peripheral forebulge of areas previously covered by ice are typically subject to monotonic RSL rise at the end of the melting due to GIA. In consequence, there is no evidence of mid or late Holocene highstand in the Caribbean, except along the northern coast of South America where the influence of far field GIA processes (ocean siphoning and continental levering) likely outweighs the influence of northward near field GIA process (subsidence in the forebulge collapse area) (Khan et al., 2017).

Simulations for quantifying GIA impact on LIG shorelines require information on the ice cover prior, during and after the LIG, thus across at least the last two glacial cycles. However, due to the very few constraints on ice cover prior to the LIG compared to the most recent deglaciation history, it is difficult to accurately quantify GIA effects over that time scale. Dendy et al. (2017) explored several models of pre-LIG ice history (varying the duration of the penultimate deglaciation, the ice mass and its spatial distribution, and the earth structure) to test the GIA signal variability and estimated an uncertainty on LIG highstand prediction that could reach up to five m for near and far field locations.

With forward modeling, Dutton and Lambeck (2012) attempted to estimate GIA magnitude for several stable sites during LIG, in far field (a priori more suitable for eustatic study) and in near field (a priori less suitable due to their greater sensitivity to the distribution of ice volume between ice sheets; a parameter which is not well constrained). Their RSL predictions for near-field sites in the Caribbean, from Bermuda to Curacao, highlighted discrepancies with observations (Dutton & Lambeck, 2012). For example, in stable Bermuda, models by Dutton and Lambeck (2012) and Muhs et al. (2020) predict paleo-sea levels ranging between 11 and 14 m above present sea level during the LIG, while LIG RSL indicators are not found above 7.4 m (Muhs et al., 2020) (Figure S7 in Supporting Information S1). Despite better constraints on GIA modeling for the period that follows the Last Glacial Maximum, estimates of the signal amplitude still suffer from large uncertainty (in the Lesser Antilles GIA estimates are at most 5 ± 5 m of RSL rise since about 6 ka, Milne & Mitrovica, 2008). In line with our present interglacial period, GIA during the LIG might have elevated the RSL in Barbuda above GMSL, allowing reefs to grow to a level higher than GMSL. Thus, a correction for GIA should lower LIG shoreline elevation in Barbuda.

Finally, a north-south gradient in elevation of the LIG highstand across the Caribbean due to GIA signal is suggested from forward modeling by Dutton and Lambeck (2012). Hence, the Yucatan, a location modeled in Dutton and Lambeck (2012), would record a smaller GIA signal than Bermuda, the Bahamas, or south Florida. According to this model, GIA signal would be of lower amplitude in Barbuda, located at lower latitude than Yucatan, Bermuda, the Bahamas, or south Florida, and thus its LIG shoreline would be less elevated by GIA than those in the northward areas (Figure S7 in Supporting Information S1).

Variation in the altitude of LIG markers over the small spatial scale across Barbuda (Russell & McIntire, 1966), as previously observed in the neighboring Guadeloupe archipelago (Battistini et al., 1986; Feuillet et al., 2004; Leclerc & Feuillet, 2019), implies an additional mechanism of crustal deformation at a smaller regional scale. Moreover, in Barbuda and in Guadeloupe elevation of the LIG markers varies along an east-west direction, in opposition to what would be expected with a contribution from GIA only (Dutton & Lambeck, 2012).

Based on the state-of-the-art understanding and modeling of GIA and DT signals, we conclude that the sum of these two mechanisms should have elevated the markers of the LIG higher in the Bahamas, south Florida and Bermuda than in Barbuda, yet the highest indicators of the past LIG RSL there are observed at similar or lower elevation than those on Barbuda (at least for Bermuda and south Florida, Figure S7 in Supporting Information S1). The comparison with the Yucatan peninsula is less easy, as GIA should be stronger than in Barbuda (Dutton & Lambeck, 2012) but DT might be weaker in northeast Yucatan Peninsula (Austermann et al., 2017) (Figure S7 in Supporting Information S1).

Since we observed LIG markers at similar or higher elevation on Barbuda than in surrounding stable areas that might have undergone stronger RSL rise from GIA and DT (Figure S7 in Supporting Information S1), we turn to local tectonic mechanisms that might have slightly uplifted the LIG shoreline on Barbuda.

5.4. Local Deformation Mechanisms

Although sedimentary processes are undoubtedly partly responsible for the general morphology of the island, the overall E-W asymmetry observed on the island might be due to a southwestward tilting of the island as previously suggested by Russell and McIntire (1966). Similar island-scale tilting with local deformation of marine terraces formed during the LIG was observed in the Guadeloupe archipelago (Battistini et al., 1986; Feuillet et al., 2004; Leclerc & Feuillet, 2019; Léticée et al., 2019).

While there are no active volcanoes on or near Barbuda that could have produced vertical deformation, the origin of this deformation may be very local due to crustal faults or more regional due to processes at the subduction interface.

5.4.1. Crustal Faults

There are two systems of faults surrounding the investigated area: active normal faults oriented N50° to E-W (Feuillet, 2000; Feuillet et al., 2002, 2010), and recently imaged N300°-trending normal faults in the forearc (Boucard et al., 2021). The first fault system might accommodate slip partitioning along the arc due the convergence obliquity (Feuillet, 2000; Feuillet et al., 2002, 2010) or bending following the entrance of the Bahamas Bank into the subduction zone during the Eocene (Legendre et al., 2018), while the second fault system would partly accommodate regional subsidence and tectonic extension in the forearc (Boucard et al., 2021).

Regarding the investigated area, several faults have been mapped offshore Barbuda, located 20 km or more from the sites discussed (Feuillet, 2000; Feuillet et al., 2002, 2010) (active faults may lie closer if they are in very shallow areas that are challenging for and have not yet been covered by marine surveys). These normal faults, which likely move at rates of a few tenths of a millimeter per year (comparable to slip rates determined for similar crustal faults on Guadeloupe, Feuillet et al., 2004; Feuillet, Beauducel, Jacques, et al., 2011), have impacts limited within a radius similar to the fault width (at most tens of kilometers) (King et al., 1988). For example, on Marie-Galante, the deformation associated with the active Morne-Piton fault rapidly decreased with distance and is negligible at 20 km from the fault (Feuillet et al., 2004). Such crustal faults are thus likely too far away to induce vertical deformation at our study sites.

No detailed study of onshore active faulting has been conducted on either Antigua or Barbuda and we therefore cannot exclude the possibility of onshore active faults within Antigua and Barbuda. The most recent study that concerns tectonics in the area is from Brown (1913) who referred to previous authors that discussed the existence of a major fault SE of Antigua, which is considered questionable by Brown (1913) who did not see any evidence of it during his survey.

Faults that cut the outer Lesser Antilles arc are all oriented N50° to E-W, while N300°-trending normal faults seem to be restricted to a transition area between the inner and the outer forearc (Boucard et al., 2021) and have not yet been reported closer to the islands. Hence, the N50° to E-W faults are likely more prone to affect Barbuda. Motion on such faults would be expected to induce NW-SE or NS gradients of deformation on the LIG shoreline elevation and not an E-W gradient.

While crustal faults might explain secondary local features, their spatial scale of impact is likely too small and their orientation (for the closest ones reported) would be unlikely to produce the deformation pattern observed. The E-W asymmetry in the island morphology, as well as differences in LIG shoreline elevation (with surrounding stable areas), might instead be due to subduction processes that may produce more regional vertical deformation.

5.4.2. Megathrust Seismic Cycle

The megathrust seismic cycle might play a role in building long-term topography. It has been documented from other subduction zones that through its seismic cycle, a megathrust fault generates a pattern of horizontal and vertical deformation in the overriding plate in response to stress accumulation and release (Chlieh et al., 2004; Savage, 1983). Long-term topography might be due to an accumulation of residual interseismic or coseismic deformation, in which case the long-term topography would mimic the coseismic or interseismic deformation

if there is a stable pattern that repeats each cycle (e.g., Melnick, 2016; Saillard et al., 2017; Taylor et al., 1980; Wesson et al., 2015).

5.4.2.1. Evidence of Recent Vertical Deformation Due To the Megathrust Seismic Cycle

Several living microatolls have been identified in the Hog Hole fringing reef and at Spanish point, on the north-east side and southern end of Barbuda, respectively (Figure 1b). Among these, which include the large one in picture 4 in Figure 1c (not sampled due to its lobate growth pattern), a smaller 1.5-m diameter *Orbicella* sp. coral microatoll was sampled and recorded submergence at about 6 mm/yr between 1953 and 2013 (Philibosian et al., 2022). This rate exceeds the regional sea-level rise recorded in the Caribbean (ranging between 1.1 ± 0.8 mm/yr and at most 3 mm/yr since 1950, Meyssignac & Cazenave, 2012; Weil-Accardo et al., 2016) and clearly indicates an additional signal to the regional sea-level rise. This residual signal suggests subsidence of the east coast of Barbuda during the 20th century due to interseismic strain accumulation on a locked portion of the megathrust interface (Philibosian et al., 2022). Such strain accumulation will be released in future earthquakes (with an inverse deformation pattern Chlieh et al., 2004), and the eastern coast that is currently subsiding might be uplifted.

This also indicates that the present elevation of the LIG terrace has been affected by interseismic subsidence since at least the last major earthquake in the area (1843 AD). Assuming a linear submergence rate of 6 mm/yr (Philibosian et al., 2022) and that the regional sea-level rise was about 1 mm/yr from 1843 to 1950 and increased to 3 mm/yr between 1950 and 2013, we estimate that the LIG RSL indicators have been lowered by 0.7 m due to interseismic subsidence. Of course, this estimate has to be taken with caution since previous studies of coral microatolls (and on other markers of vertical deformation) have highlighted that deformation rates can change over short timescales due to coupling variability of the megathrust (e.g., Meltzner et al., 2015; Philibosian et al., 2014; Weil-Accardo et al., 2016, 2020).

Since deformation related to a megathrust seismic cycle varies along a transect perpendicular to the trench, with interseismic subsidence observed close to the trench and uplift further away (Chlieh et al., 2004), interseismic uplift might be expected westward of the area experiencing interseismic subsidence. Unfortunately, there are no coral microatolls on the west coast of Barbuda with which to easily compare RSL changes, perhaps due to local variations in hydrodynamics and sediment supply driven by prevailing winds that might be detrimental to coral development.

Looking for other RSL indicators on Barbuda, we noted submerged beachrocks around Goat Point, in the north-east (Figure 1c picture 3). These beachrocks might be the mark of the continuous Holocene sea-level rise since about 6 ka due to GIA and/or related to tectonic subsidence (sudden or gradual). However, present sea level would have been reached around 4,085 years BP (Brasier & Donahue, 1985; Brasier & Mather, 1975), according to radiocarbon dating of a slightly elevated limestone ridge on the west side of Barbuda that is filled with *Strombus* fragments and is interpreted as a shoreline deposit (Watters et al., 1992). Since the Goat Point beachrocks are not dated, they might also represent a more recent RSL rise (similar to those affecting coral microatolls) as suggested by Russell and McIntire (1966).

Located close to Palmetto Point in the southwest part of the island, the now-ruined Martello tower (location in Figure 1b) was built about 200 years ago and presumably sited close to the shore (Harris, 1965; Russell & McIntire, 1966). Today, it is located about 250 m inland, a distance that increased since the publication of Harris (1965), who estimated a distance of about 100 m from the shoreline. According to Harris (1965) and Russell and McIntire (1966), this change is primarily due to the Late Holocene seaward progradation of the Palmetto Point beach ridges, although Russell and McIntire (1966) also briefly mentioned crustal deformation as acting on the Holocene accretionary topography at Palmetto Point. Coastal progradation is mainly controlled by sediment influx and RSL changes. While RSL rise will generally lead to coastal retreat, abundant sediment influx might balance and even overtake RSL rise and lead to coastal progradation. Likewise, RSL decrease combined to sediment influx could explain coastal progradation. Without quantification of sediment influx in Palmetto Point, it remains difficult to characterize RSL changes there.

Comparison of historic charts and maps suggests a high rate of beach ridge progradation between 1750 and 1992 (Watters et al., 1992), with at least one beach ridge built in the area between 1958 and 1964 (according to aerial photographs Russell & McIntire, 1966). During this period, the major subduction earthquake (8 February 1843) occurred offshore Antigua and Guadeloupe with an estimated magnitude of 8.5 (Feuillet, Beauducel, &

Tapponnier, 2011; Hough, 2013; McCann & Sykes, 1984). Despite an estimated intensity of IX in Antigua, no vertical deformation was documented and only collapse of coastal cliffs and a possible tsunami were reported there (Bernard & Lambert, 1988). Unfortunately, no study of ground deformation was conducted on the remote Barbuda island after the earthquake. The very large boulders observed on the Codrington terrace that fell from the above terrace might be evidence of strong shaking in a major subduction earthquake, or simply due to erosion. The observation of a paleo-notch at the base of a few of these boulders (Figure S5 in Supporting Information S1) implies that they fell longer ago, before the 1843 earthquake.

The lack of evidence for crustal deformation on the west coast of Barbuda suggests that wind and sand supply might be the main explanations for the dune progradation and for the inland position of the Martello tower as suggested by Brasier and Donahue (1985) and that the tectonic signal, if any, might be small and hidden by beach ridge dynamics.

The study of coral microatolls in Antigua documents RSL changes westward of Barbuda. Submergence rates inferred from one sampled microatoll indicate a drastic decrease around 1980 from 9 mm/yr to at most 2 mm/yr, perhaps due to a change in location or degree of megathrust coupling (Philibosian et al., 2022). Thus, for the last several decades, eastern Barbuda seems to have submerged faster than its westward neighboring island, in agreement with the expected trench-perpendicular deformation pattern.

The topography of Barbuda, emergent on the east and submergent on the west, is the opposite of the pattern suggested by shorter-term observations with cup-shaped microatolls and submerged beachrocks on the east and a lack of RSL rise observations on the west. The topography of Barbuda could therefore be related to successive earthquakes whose vertical deformation patterns would be the inverse of the current interseismic pattern. In this scenario, the coseismic deformation would not be fully compensated by the following interseismic deformation and residual deformation would accumulate over time (e.g., Taylor et al., 1987).

5.4.2.2. Downdip Limit of the Seismogenic Zone

Such lack of compensation of short-term seismic cycle deformation has been observed elsewhere, as in western Myanmar (Wang et al., 2013) or in the Solomon islands (e.g., Thirumalai et al., 2015) with a long-term topography that mimics pattern of coseismic deformation.

Considering such a scenario, we attempt to use the long-term deformation pattern to locate the lower limit of seismogenic locking on the megathrust (Figure 5). It is well known that this limit lies below the hinge line which separates areas undergoing subsidence from those recording uplift during an earthquake (Figure 5) (Chlieh, 2003). The location of this hinge line may be stable over the long term and may separate areas of long-term subsidence from those of long-term uplift. In that case, the present topography of the island suggests that it would pass through the middle of Barbuda.

From the refined slab geometry (outlined by relocated seismicity) of Bie et al. (2020), the slab is about 50 km below the hinge line running through Barbuda implying that the downdip limit of the seismogenic zone (and thus the megathrust) may be as deep as 50 km, while it lies deeper below the hinge line between Grande-Terre and Basse-Terre in the Guadeloupe archipelago (Figure 5) and in Martinique (locking depth proposed at 60 km, Weil-Accardo et al., 2016). Interestingly, we also note that the slab is found about 50 km below both eastern Barbuda and La Désirade islands, which share similar maximum elevations for their LIG shorelines. The corresponding seismogenic zone would hence extend below the Moho (Figure 5), as proposed by previous studies based on seismicity (Bie et al., 2020; Laigle et al., 2013; Ruiz et al., 2013) and coral microatolls (Philibosian et al., 2022; Weil-Accardo et al., 2016).

The accumulation of residual short-term deformation over millennia might be related to the deep seismicity below the Moho, similarly to observations made along the central Andean coast where long-term deformation mimics coseismic deformation generated during deep earthquakes straddling the crust-mantle limit (Melnick, 2016). Also, the Barracuda Ridge which is subducting below Barbuda is another possible driver of long-term deformation, given the several instances of vertical deformation due to ridge subduction that have been noted elsewhere, such as in Peru with the Nazca Ridge (Macharé & Ortlieb, 1992) and Vanuatu with the Entrecasteaux Ridge (Taylor et al., 1987, 1990). In the Solomon islands, for example, the comparison between records of vertical deformation at three timescales (coral microatolls for short-term deformation, Holocene emerged reef flat, and long-term topography) highlighted that some sites were recording a slow continuous uplift that tends to

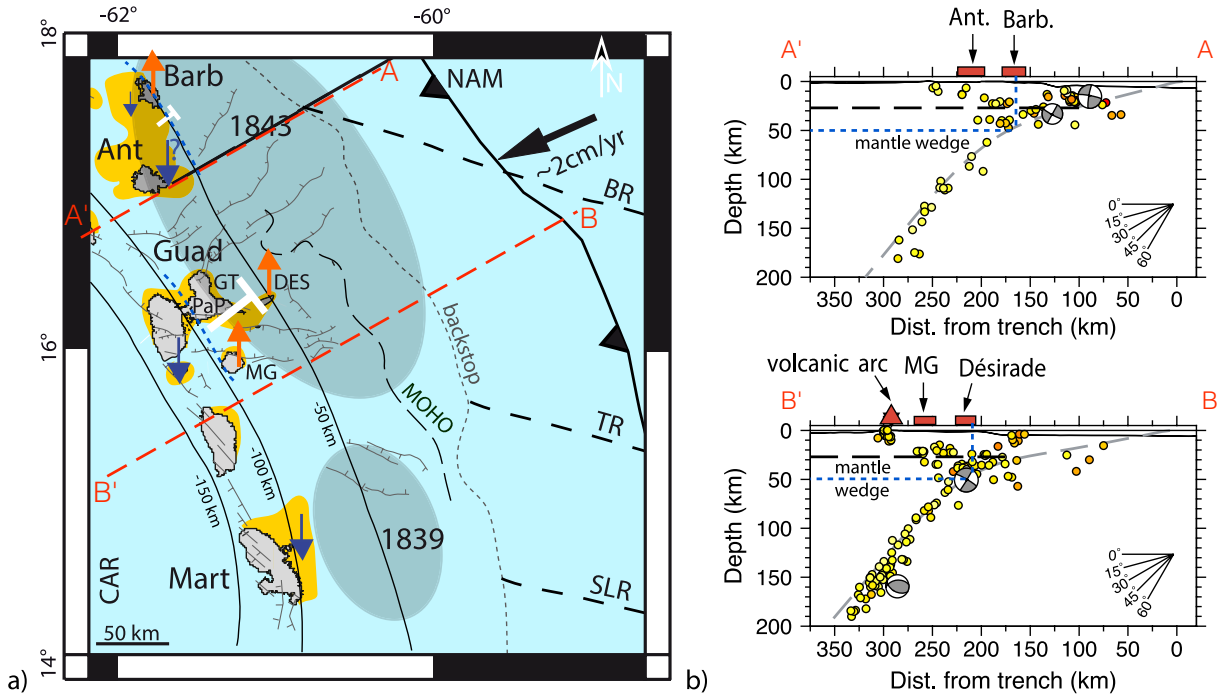

Figure 5. Long-term deformation throughout the Lesser Antilles arc and downdip limit of the seismogenic zone. (a) Tectonic setting. BR: Barracuda ridge, TR: Tiburon ridge, SLR: St. Lucia ridge. NAM, CAR: North American, Caribbean Plates. Barb: Barbuda, Ant: Antigua, Guad: Guadeloupe archipelago, Mart: Martinique. GT: Grande-Terre, MG: Marie-Galante, DES: Désirade island, PaP: Point-a-Pitre location in Guadeloupe. Active crustal faults in gray from Feuillet (2000), Feuillet et al. (2002, 2004), Feuillet, Beauducel, Jacques, et al. (2011), Leclerc (2014). Gray ellipses: rupture areas for 1839 M8 and 1843 M8.5 earthquakes (Feuillet, Beauducel, Jacques, et al., 2011). Orange areas: submarine carbonate platforms. Black barbed line: accretionary prism frontal thrust. Dashed gray line: primary negative gravity anomaly corresponding to the Lesser Antilles backstop (Bowin, 1976; Evain et al., 2013; Laigle et al., 2013; Westbrook et al., 1988). Black contours depict slab geometry from Bie et al. (2020). Dashed black line: Moho from Paulatto et al. (2017). White T: apparent southwestward tilting of Barbuda (mainly based on its morphology) and of the Guadeloupe archipelago (Feuillet et al., 2004). Orange arrows: long-term uplift. Blue arrows: long-term subsidence. Dashed blue line: proposed hinge line between areas experiencing long-term uplift and subsidence. Dashed red lines: locations of profiles in part (b). (b) Sectional views of the subduction zone from the trench to the volcanic arc adapted from Bie et al. (2020). Gray dashed curves: slab interfaces from Bie et al. (2020). Projected locations of Antigua and Barbuda islands and of the Guadeloupe archipelago islands are indicated. Dashed blue line: proposed hinge line.

reduce the amplitude of interseismic subsidence and leads to permanent uplift that mimics coseismic deformation (Thirumalai et al., 2015). The sites' alignment with the Simbo ridge axis might indicate its role in building forearc permanent deformation (Thirumalai et al., 2015).

5.5. Long-Term Uplift

In addition to the well-dated LIG terrace, higher terraces and notches are observed along the eastern coast of Barbuda at Two Foot Bay. Although we have no age constraints on these higher paleo-sea levels, they may result from interplay between long-term tectonic uplift and Quaternary eustatic sea-level variations as observed along many coasts in active areas worldwide (e.g., Armijo et al., 1996), instead of being the result of progressive sea-level falling since the Pliocene (Brasier & Donahue, 1985; Brasier & Mather, 1975). In this section, we speculate about possible ages for the higher terraces and their implications for the history of uplift.

Marine reef terraces grow underwater on a preexisting topographic slope (basement); the shallower the slope, the wider the terrace (Leclerc & Feuillet, 2019; Toomey et al., 2013). At Two Foot Bay, the present fringing reef is very narrow, likely developing on a very steep insular slope. In that condition, it may be difficult to build and preserve a set of uplifted marine reef terraces. Mostly abrasion notches carved into the cliff may have been preserved as markers of paleo-sea levels. In such conditions, it is difficult to firmly establish the chronology of those paleo-sea levels.

Although the age of the lower sedimentary unit composing the Highland Formation is well known (Brasier & Mather, 1975; Cornee et al., 2021), the upper surface of the formation is highly weathered (Cornee et al., 2021)

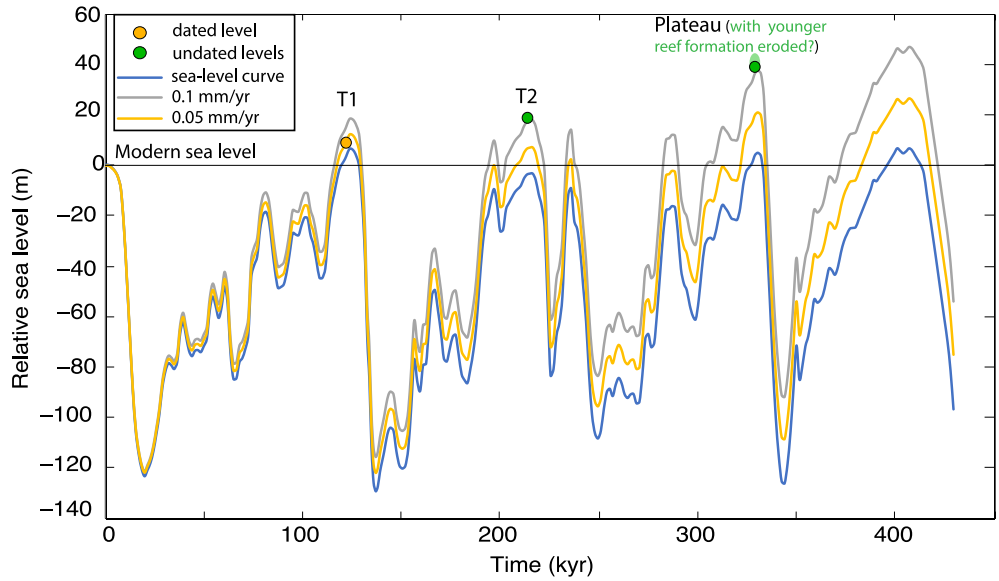

Figure 6. Uplift rate calculation assuming that upper terraces correspond to previous interglacials. Using the sea-level curve of Waelbroeck et al. (2002) (blue curve), we applied a long-term uplift of 0.05 mm/yr (yellow curve) and 0.1 mm/yr (gray curve) to match present elevations of the terraces. T1 is dated to the Last Interglacial (orange dot), the terrace T2 (green dot) is assumed to represent marine isotope stage 7 (MIS 7) (≈215 ka), and a hypothetical eroded deposit (green dot that marks the highest elevation of the plateau and a lighter green ellipse that represents the upper younger reef formation that might have been fully eroded) that would have lain atop the plateau is assumed to represent MIS 9 (≈330 ka). Like T1, terrace T2 is marked by a paleo abrasion notch, so we corrected its elevation in a similar way as we did for T1 and inferred a paleo relative sea-level of 17 m. For the plateau, we used its maximum elevation of 39 m on the topographic map (Figure 1b), since it is a planed-off surface that might have undergone significant erosion. In this scenario, the elevation of T1 corresponds to an uplift rate of 0.05 mm/yr, while a higher uplift rate (≈0.1 mm/yr) would better fit the elevations of T2 and the plateau. These rates should be considered as maximum estimates, since they are not corrected for potential uplift due to glacial isostatic adjustment or dynamic topography.

rendering the identification and the dating of the foraminifera assemblage difficult, with large age uncertainty (see Appendix H from the supplementary material of Cornee et al., 2021). Hence, this upper formation may be 2.5 Ma old (Cornee et al., 2021), but we cannot exclude the possibility that the upper part of the formation was in part eroded. The foraminifera assemblages of the Highland Formation indicate that it was formed at depth ranging between 20 and 100 m (Brasier & Mather, 1975; Cornee et al., 2021). In a context of uplift during the Quaternary, such a formation may have been brought closer to the sea surface and fringed by reef patches that were not preserved after the emersion due to subaerial erosion.

Assuming that in Barbuda, the present LIG terrace elevation is partly uplifted by tectonics and using correlation with the curve of eustatic sea-level change of Waelbroeck et al. (2002), we can estimate an uplift rate of about 0.05 mm/yr since 125 ka (Figure 6). Coastlines that are uplifted at such slow rates record only the main sea-level highstands, which correspond to interglacials (e.g., Armijo et al., 1996; Feuillet et al., 2004, and references therein). In keeping with this hypothesis, we infer that all markers of paleo-sea level we have observed at Two Foot Bay (terraces and notches) were likely also formed during interglacial periods at sea levels that differ by at most few meters from the present-day sea level. We used the curve of eustatic sea-level change of Waelbroeck et al. (2002) to correlate our markers of paleo-sea level with previous interglacial highstands (Figure 6). The second major marine terrace T2 which could be either a constructional reef or an abrasion platform might have been formed during the marine isotopic stage 7 (≈215 ka). The deep notch above T2 was likely carved during the same interglacial period. The upper plateau of Barbuda, which is the only extensive surface above T2, lying about 39 m above the present sea level, might have emerged during the previous isotopic stage 9 (≈330 ka). Such a hypothesis for the ages of formation of T2 and emergence of the Plateau of Barbuda implies that the morphology of Barbuda Island was shaped during the Quaternary by tectonics as previously suggested by Martin-Kaye (1959), Harris (1965), Russell and McIntire (1966). Indeed, given the present altitude of those paleo sea-level markers (notch and top of the plateau), the tectonic uplift rate would have been slow and approximately constant over the

past 330 ka (between 0.05 and 0.1 mm/yr) (Figure 6). However, we cannot exclude different ages for undated levels and this would impact the uplift rates before the isotopic stage 5.

6. Conclusions

Following pioneering work conducted on Barbuda up to the 1990s, recent work of Cornee et al. (2021), and thanks to the last few decades' advances in both geochronology and surveying, we started to reinvestigate a set of emergent marine terraces on the eastern coast of the island. We performed the first U-Th ages by MC-ICPMS and made accurate elevation measurements using a TS. We conclude without ambiguity that there are two types of RSL indicators at the site, a fossil reef at an elevation of 5 ± 0.5 m above modern MSL and an abrasion notch at 9 ± 1 m above modern MSL, both related to LIG paleo-sea level dated between 122.8 ± 0.3 ka and 128.1 ± 0.3 ka (2σ). By estimating the elevations of modern analogs of the two RSL indicators, we calculate consistent paleo-RSL values for the LIG shoreline on the east coast of Barbuda with an average of 7 ± 2 m of elevation above MSL. The comparison with LIG RSL indicators in surrounding stable areas along with the spatial scale and gradient of regional to local non-tectonic signals (eustatic sea level, GIA, and DT) allowed us to estimate the relative impact of each process on the present elevation of LIG shorelines from Barbuda to northward stable areas such as the Bahamas and Bermuda. This leads us to infer regional tectonics as a fourth source of RSL change in Barbuda, as suggested by a few previous authors (Harris, 1965; Martin-Kaye, 1959; McCann & Sykes, 1984; Russell & McIntire, 1966). The possible southwestward tilting of Barbuda inferred from its general morphology, combined with the difference in LIG shoreline elevation between Antigua and Barbuda, is reminiscent of the E-W gradient in vertical deformation observed throughout the Guadeloupe archipelago (Feuillet et al., 2004; Leclerc & Feuillet, 2019) and is suggestive of a common, regional source of land-level change. While active crustal faults could explain minor, local deformation, their general orientation through the arc (at least for the closest known set of faults, Feuillet et al., 2004) is not compatible with the E-W gradient in LIG shoreline elevation. Volcanoes are too distant to generate deformation on Barbuda. Thus, the subduction megathrust appears to be the most likely source of vertical deformation on Barbuda. The presence of cup-shaped microatolls on the eastern reef of Barbuda that are recording subsidence, likely related to interseismic coupling on the megathrust interface (Philibosian et al., 2022), suggests that long-term vertical deformation might be generated through the accumulation of residual coseismic deformation. The corresponding edge of the seismogenic zone would extend into the mantle wedge corner, as proposed by previous studies based on seismicity (Bie et al., 2020; Laigle et al., 2013; Ruiz et al., 2013) and coral microatolls (Philibosian et al., 2022; Weil-Accardo et al., 2016).

Although we cannot firmly conclude how tectonics are affecting Barbuda, we gather a set of evidence that suggests a non-negligible RSL signal related to a plate-scale process. Dating the terrace T2 of Barbuda would help to constrain tectonics before the LIG (accurately calculate the uplift rate and assess its stability over time). Also, dating the drowned beachrocks observed on the northern tip of Barbuda (that might indicate century-scale interseismic RSL rise similar to that recorded by microatolls, sudden coseismic subsidence events or a Holocene SL rise due to GIA) could help to extend the microatoll record into the past, constraining RSL changes and possible coupling variability of the megathrust interface (as highlighted elsewhere, Meltzner et al., 2015; Philibosian et al., 2014; Philibosian et al., 2022; Weil-Accardo et al., 2016, 2020).

Finally, extending the study of the submerged reef platforms (as it has been done in Les Saintes and Martinique, Leclerc et al., 2014; Leclerc et al., 2015) to Antigua-Barbuda, would help to more thoroughly explore long-term tectonics and active crustal faulting in this northern part of the Lesser Antilles arc. Extensive onshore scouting in Antigua is needed, as well as dating of the eroded limestone unit between Willoughby and Mamora Bays on SE Antigua to better constrain the history of RSL changes in Antigua and connect it to that of Barbuda. Lastly, future advances in GIA and DT modeling at local scale will help to quantitatively disentangle all the post-depositional processes that have affected LIG shorelines since their formation in the Lesser Antilles arc.

Appendix A: U/Th Dating of Corals

The chemical and analytical procedures consisting of separating and purifying uranium followed by thorium from the calcium matrix prior to isotope ratio measurements were carried out at CEREGE. The sample is first dissolved with nitric acid. Then, the sample is spiked with a ^{229}Th-^{233}U-^{236}U in-house mixture and allowed to equilibrate. After equilibration, dissolved iron is added to the sample and the pH of the solution is raised to about

8 by adding NH_4OH to coprecipitate uranium and thorium with iron oxy-hydroxides. Uranium and thorium are then separated by extraction chromatography using columns with UTEVA resin. Sample/spike ratios were 8.8 ± 2.3 (1σ) for $^{235}U/^{233}U$ and 0.21 ± 0.05 (1σ) for $^{230}Th/^{229}Th$. For each batch of 11 samples a spiked procedural blank was prepared.

Analyses were conducted on a MC-ICPMS NEPTUNE PLUS following the procedure of Chiang et al. (2019). Briefly, sample solutions diluted in 1% HNO_3 (with traces of HF) were introduced in the mass spectrometer (MS) in dry plasma mode using an Apex Omega HF and a 100 µL/min Opalmist nebulizer. The MS was equipped with a Ni Jet sample cone and a Ni H skimmer cone. The daily sensitivity was about 400 V/ppm for U and Th. The U and Th fractions of each sample were analyzed separately. U fractions were analyzed at about 0.8 V of ^{238}U by peak jumping of ^{233}U, ^{234}U, ^{235}U, ^{236}U on the central SEM equipped with a Retarding Potential Quadrupole (RPQ). Each analysis consisted of 1 block of 600 cycles (which resulted in about 3 mL of sample consumption). Th fractions were analyzed at about 200 kcps of ^{229}Th by peak jumping of ^{229}Th and ^{230}Th on the central SEM equipped with an RPQ. ^{232}Th was monitored on a Faraday cup for each cycle. Each analysis consisted in 1 block of 450 cycles (which resulted in about 2 mL of sample consumption).

For each daily session of analyses (U or Th), abundance sensitivity and hydrides were monitored at mass 237 and 239 on the SEM + RPQ (respectively around 250 and 700 ppb) using a 2V ^{238}U beam at the beginning and end of each batch. Data were processed by correcting for SEM dark noise (measured every day), dead time, and on-peak blanks using the Thermo Software. Then, abundance sensitivity, hydrides, peak-jumping beam time-interpolation, instrumental mass bias (for Th, the instrumental mass bias was corrected using multiple analyses of a spiked U SRM960 solution assuming that it is identical for Th and U), contributions from the spike and procedural blanks as well as error propagation were processed using an in-house Microsoft Excel v.16.46 (Microsoft Corporation, Redmond, WA) macro.

Spiked HU-1 processed through the same procedure as the sample was analyzed multiple times to check for accuracy. Average results of HU-1 for this study were: ($^{234}U/^{238}U$) = 0.999 ± 0.001 (2SD, n = 8); ($^{230}Th/^{238}U$) = 1.004 ± 0.002 (2SD, n = 10), in good agreement with published values (Cheng et al., 2013).

Finally, $^{230}Th/^{238}U$ ages were obtained using Isoplot-R (option U-Series/ages) (Vermeesch, 2018).

Data Availability Statement

Data are included in the main text and supporting information file as figures. Any additional information (total station data, kinematic Global Positioning System data) can be found here: http://doi.org/10.6084/m9.figshare.15001014.

Acknowledgments
We are very grateful to the Survey Department of Antigua-Barbuda who provided access to aerial images of the two islands that were very helpful for our fieldwork. Our field survey would have not been possible without our great host Serene who took care of us during our stays onshore in 2009 and 2012. We also thank Frederique, her husband and their children living on this remote island for their logistical help. Brian Atwater and Bob Halley assisted with field logistics in 2013. We thank Jacqueline Austermann for her valuable help in understanding how the DT might have changed the elevation of the LIG shoreline in Barbuda and Frederique Leclerc for her valuable proofreading and comments. Helene Mariot and Marion Defrance are thanked for their careful maintenance of CEREGE's clean laboratory. We would also like to thank Daniel Muhs, James Joyce and Jean-Jacques Cornée whose comments improved the clarity of the manuscript. The project leading to this publication received funding from the French ANR (project SUBSISMANTI ANR-05-CATT-0015, project CARQUAKES ANR17-CE03-0006), INSU (program ALEAS) and from two French ANR "Investissement d'avenir" programs through the EQUIPEX ASTER-CEREGE and the DATCARB project from the "Excellente initiative" program of Aix Marseille University A*MIDEX. JWA is supported by a post-doctoral grant of the French National Research Institute for Sustainable Development (IRD). BP was supported by an AXA Postdoctoral Fellowship (PDOC-2012-W1). Any use of trade, firm, or product names is for descriptive purposes only and does not imply endorsement by the U.S. Government.

References

Agnew, D. C. (2012). *SPOTL: Some programs for ocean-tide loading*. Retrieved from https://escholarship.org/uc/item/954322pg

Andersen, M., Stirling, C., Zimmermann, B., & Halliday, A. (2010). Precise determination of the open ocean $^{234}U/^{238}U$ composition. *Geochemistry, Geophysics, Geosystems*, *11*(12), Q12003. https://doi.org/10.1029/2010gc003318

Andreieff, P., Bouysse, P., & Westercamp, D. (1987). *Géologie de L'arc Insulaire Des Petites Antilles Et Évolution Géodynamique De l'Est-Caraïbe*. (Unpublished doctoral dissertation), (Vol. 1).

Armijo, R., Meyer, B., King, G., Rigo, A., & Papanastassiou, D. (1996). Quaternary evolution of the Corinth Rift and its implications for the Late Cenozoic evolution of the Aegean. *Geophysical Journal International*, *126*(1), 11–53. https://doi.org/10.1111/j.1365-246x.1996.tb05264.x

Austermann, J., Mitrovica, J. X., Huybers, P., & Rovere, A. (2017). Detection of a dynamic topography signal in Last Interglacial sea-level records. *Science Advances*, *3*(7), e1700457. https://doi.org/10.1126/sciadv.1700457

Bain, A., Kennedy, L., Burn, M., & Faucher, A.-M. (2010). *Field report archaeobotany, palaeoclimatology and archaeoentomology in Barbuda*.

Barlow, N. L., McClymont, E. L., Whitehouse, P. L., Stokes, C. R., Jamieson, S. S., Woodroffe, S. A., et al. (2018). Lack of evidence for a substantial sea-level fluctuation within the Last Interglacial. *Nature Geoscience*, *1*(9), 627–634. https://doi.org/10.1038/s41561-018-0195-4

Battistini, R., Hinschberger, F., Hoang, C., & Petit, M. (1986). La basse terrasse corallienne Pleistocene (Eemien) de la Guadeloupe: Morphologie, datations $^{230}Th/^{234}U$, neotectonique. *Revue de Geomorphologie Dynamique*, *25*(1), 1–10.

Bernard, P., & Lambert, J. (1988). Subduction and seismic hazard in the northern Lesser Antilles: Revision of the historical seismicity. *Bulletin of the Seismological Society of America*, *78*(6), 1965–1983.

Bie, L., Rietbrock, A., Hicks, S., Allen, R., Blundy, J., Clouard, V., et al. (2020). Along-Arc heterogeneity in local seismicity across the Lesser Antilles Subduction Zone from a dense Ocean-Bottom Seismometer network. *Seismological Research Letters*, *91*(1), 237–247. https://doi.org/10.1785/0220190147

Biguenet, M., Sabatier, P., Chaumillon, E., Chagué, C., Arnaud, F., & Feuillet, N. (2020). Sedimentary records of tsunamis and hurricanes in the Lesser Antilles. *Agu fall meeting abstracts*, *2020*, NH004.

Blanchon, P. (2011). Geomorphic zonation. *Encyclopedia of modern coral reefs*, 469–486. https://doi.org/10.1007/978-90-481-2639-2_33

Blanchon, P., Eisenhauer, A., Fietzke, J., & Liebetrau, V. (2009). Rapid sea-level rise and reef back-stepping at the close of the Last Interglacial highstand. *Nature*, *458*(7240), 881–884. https://doi.org/10.1038/nature07933

Boucard, M., Marcaillou, B., Lebrun, J.-F., Laurencin, M., Klingelhoefer, F., Laigle, M., et al. (2021). Paleogene V-shaped basins and Neogene subsidence of the Northern Lesser Antilles Forearc. *Tectonics*, *40*(3), e2020TC006524. https://doi.org/10.1029/2020tc006524

Bowin, C. (1976). *Caribbean Gravity Field and Plate Tectonics* (Vol. 169). Geological Society of America.

Brasier, M., & Donahue, J. (1985). Barbuda—An emerging reef and lagoon complex on the edge of the Lesser Antilles island are. *Journal of the Geological Society*, *142*(6), 1101–1117. https://doi.org/10.1144/gsjgs.142.6.1101

Brasier, M., & Mather, J. (1975). The stratigraphy of Barbuda, West Indies. *Geological Magazine*, *112*(3), 271–282. https://doi.org/10.1017/s0016756800047026

Brown, A. P. (1913). *Notes on the geology of the island of Antigua* (pp. 584–616). Proceedings of the Academy of Natural Sciences of Philadelphia.

Carpenter, K. E., Abrar, M., Aeby, G., Aronson, R. B., Banks, S., Bruckner, A., et al. (2008). One-third of reef-building corals face elevated extinction risk from climate change and local impacts. *Science*, *321*(5888), 560–563. https://doi.org/10.1126/science.1159196

Chappell, J. (1974). Geology of coral terraces, Huon peninsula, New Guinea: A study of Quaternary tectonic movements and sea-level changes. *The Geological Society of America Bulletin*, *85*(4), 553–570. https://doi.org/10.1130/0016-7606(1974)85<553:gocthp>2.0.co;2

Charter, C. F. (1937). Soil survey (reconnaissance) of Antigua and Barbuda, Leeward Islands. *Soil Survey (reconnaissance) of Antigua and Barbuda*.

Chen, T., Robinson, L. F., Beasley, M. P., Claxton, L. M., Andersen, M. B., Gregoire, L. J., et al. (2016). Ocean mixing and ice-sheet control of seawater $^{234}U/^{238}U$ during the last deglaciation. *Science*, *354*(6312), 626–629. https://doi.org/10.1126/science.aag1015

Cheng, H., Edwards, R. L., Shen, C.-C., Polyak, V. J., Asmerom, Y., Woodhead, J., et al. (2013). Improvements in ^{230}Th dating, ^{230}Th and ^{234}U half-life values, and U–Th isotopic measurements by multi-collector inductively coupled plasma mass spectrometry. *Earth and Planetary Science Letters*, *371*, 82–91. https://doi.org/10.1016/j.epsl.2013.04.006

Chiang, H.-W., Lu, Y., Wang, X., Lin, K., & Liu, X. (2019). Optimizing MC-ICP-MS with SEM protocols for determination of U and Th isotope ratios and ^{230}Th ages in carbonates. *Quaternary Geochronology*, *50*, 75–90. https://doi.org/10.1016/j.quageo.2018.10.003

Chlieh, M. (2003). *Le cycle sismique décrit avec les données de la géodésie spatiale (interférométrie sar et gps différentiel): Variations spatio-temporelles des glissements stables et instables sur l'interface de subduction du nord chili (unpublished doctoral dissertation)*. Institut de physique du globe.

Chlieh, M., De Chabalier, J., Ruegg, J., Armijo, R., Dmowska, R., Campos, J., & Feigl, K. (2004). Crustal deformation and fault slip during the seismic cycle in the North Chile subduction zone, from GPS and InSAR observations. *Geophysical Journal International*, *158*(2), 695–711. https://doi.org/10.1111/j.1365-246x.2004.02326.x

Chutcharavan, P. M., Dutton, A., & Ellwood, M. J. (2018). Seawater $^{234}U/^{238}U$ recorded by modern and fossil corals. *Geochimica et Cosmochimica Acta*, *224*, 1–17. https://doi.org/10.1016/j.gca.2017.12.017

Cornee, J.-J., Münch, P., Philippon, M., Boudagher-Fadel, M., Quillévéré, F., Melinte-Dobrinescu, M., et al. (2021). Lost islands in the northern Lesser Antilles: Possible milestones in the Cenozoic dispersal of terrestrial organisms between South-America and the Greater Antilles. *Earth-Science Reviews*, *217*, 103617. https://doi.org/10.1016/j.earscirev.2021.103617

Dávila, F. M., & Lithgow-Bertelloni, C. (2013). Dynamic topography in South America. *Journal of South American Earth Sciences*, *43*, 127–144. https://doi.org/10.1016/j.jsames.2012.12.002

DeMets, C., Jansma, P. E., Mattioli, G. S., Dixon, T. H., Farina, F., Bilham, R., et al. (2000). GPS geodetic constraints on Caribbean-North America plate motion. *Geophysical Research Letters*, *27*(3), 437–440. https://doi.org/10.1029/1999gl005436

De Min, L., Lebrun, J.-F., Cornée, J.-J., Münch, P., Léticée, J., Quillévéré, F., et al. (2015). Tectonic and sedimentary architecture of the Karukéra spur: A record of the Lesser Antilles fore-arc deformations since the Neogene. *Marine Geology*, *363*, 15–37. https://doi.org/10.1016/j.margeo.2015.02.007

Dendy, S., Austermann, J., Creveling, J., & Mitrovica, J. (2017). Sensitivity of Last Interglacial sea-level high stands to ice sheet configuration during Marine Isotope Stage 6. *Quaternary Science Reviews*, *171*, 234–244. https://doi.org/10.1016/j.quascirev.2017.06.013

Deschamps, P., Durand, N., Bard, E., Hamelin, B., Camoin, G., Thomas, A. L., et al. (2012). Ice-sheet collapse and sea-level rise at the Bølling warming 14,600 years ago. *Nature*, *483*(7391), 559–564. https://doi.org/10.1038/nature10902

Donovan, S. K., Jackson, T. A., Harper, D. A., Portell, R. W., & Renema, W. (2014). The Upper Oligocene of Antigua: The volcanic to limestone transition in a limestone Caribbee. *Geology Today*, *30*(4), 151–158. https://doi.org/10.1111/gto.12061

Dutton, A., Carlson, A. E., Long, A., Milne, G. A., Clark, P. U., DeConto, R., et al. (2015). Sea-level rise due to polar ice-sheet mass loss during past warm periods. *Science*, *349*(6244), aaa4019. https://doi.org/10.1126/science.aaa4019

Dutton, A., & Lambeck, K. (2012). Ice volume and sea level during the Last Interglacial. *Science*, *337*(6091), 216–219. https://doi.org/10.1126/science.1205749

Dutton, A., Webster, J. M., Zwartz, D., Lambeck, K., & Wohlfarth, B. (2015). Tropical tales of polar ice: Evidence of Last Interglacial polar ice sheet retreat recorded by fossil reefs of the granitic Seychelles islands. *Quaternary Science Reviews*, *107*, 182–196. https://doi.org/10.1016/j.quascirev.2014.10.025

Edwards, R., Gallup, C., & Cheng, H. (2003). Uranium-series dating of marine and lacustrine carbonates. *Reviews in Mineralogy and Geochemistry*, *52*(1), 363–405. https://doi.org/10.2113/0520363

Evain, M., Galve, A., Charvis, P., Laigle, M., Kopp, H., Bécel, A., et al. (2013). Structure of the Lesser Antilles subduction forearc and backstop from 3D seismic refraction tomography. *Tectonophysics*, *603*, 55–67. https://doi.org/10.1016/j.tecto.2011.09.021

Feuillard, M. (1985). *Macrosismicité de la Guadeloupe et de la Martinique*. Observatoire volcanologique de la Soufrière. (Guadeloupe).

Feuillet, N. (2000). *Sismotectonique des Petites Antilles: Liaison entre activité sismique et volcanique* (Unpublished doctoral dissertation). (Vol. 7).

Feuillet, N., Beauducel, F., Jacques, E., Tapponnier, P., Delouis, B., Bazin, S., et al. (2011). The Mw = 6.3, November 21, 2004, Les Saintes earthquake (Guadeloupe): Tectonic setting, slip model and static stress changes. *Journal of Geophysical Research*, *116*(B10), B10301. https://doi.org/10.1029/2011jb008310

Feuillet, N., Beauducel, F., & Tapponnier, P. (2011). Tectonic context of moderate to large historical earthquakes in the Lesser Antilles and mechanical coupling with volcanoes. *Journal of Geophysical Research*, *116*(B10), B10308. https://doi.org/10.1029/2011jb008443

Feuillet, N., Leclerc, F., Tapponnier, P., Beauducel, F., Boudon, G., Le Friant, A., et al. (2010). Active faulting induced by slip partitioning in Montserrat and link with volcanic activity: New insights from the 2009 GWADASEIS marine cruise data. *Geophysical Research Letters*, *37*(19), L00E15. https://doi.org/10.1029/2010gl042556

Feuillet, N., Manighetti, I., Tapponnier, P., & Jacques, E. (2002). Arc parallel extension and localization of volcanic complexes in Guadeloupe, Lesser Antilles. *Journal of Geophysical Research*, *107*(B12). ETG–3. https://doi.org/10.1029/2001jb000308

Feuillet, N., Tapponnier, P., Manighetti, I., Villemant, B., & King, G. (2004). Differential uplift and tilt of Pleistocene reef platforms and Quaternary slip rate on the Morne-Piton normal fault (Guadeloupe, French West Indies). *Journal of Geophysical Research*, *109*(B2), B02404. https://doi.org/10.1029/2003jb002496

Harris, D. (1965). *Plants, animals and man in the outer leeward island, west indies* (p. 131). MC Kellman, Plant GeographyMethuen & Co. Ltd.

Hearty, P. J., Hollin, J. T., Neumann, A. C., O Leary, M. J., & McCulloch, M. (2007). Global sea-level fluctuations during the Last Interglaciation (MIS 5e). *Quaternary Science Reviews*, *26*(17–18), 2090–2112. https://doi.org/10.1016/j.quascirev.2007.06.019

Hibbert, F. D., Rohling, E. J., Dutton, A., Williams, F. H., Chutcharavan, P. M., Zhao, C., & Tamisiea, M. E. (2016). Coral indicators of past sea-level change: A global repository of U-series dated benchmarks. *Quaternary Science Reviews*, *145*, 1–56. https://doi.org/10.1016/j.quascirev.2016.04.019

Hill, D. F. (2016). Spatial and temporal variability in tidal range: Evidence, causes, and effects. *Current Climate Change Reports*, *2*(4), 232–241. https://doi.org/10.1007/s40641-016-0044-8

Hough, S. E. (2013). Missing great earthquakes. *Journal of Geophysical Research: Solid Earth*, *118*(3), 1098–1108. https://doi.org/10.1002/jgrb.50083

Jaffey, A., Flynn, K., Glendenin, L., Bentley, W. t., & Essling, A. (1971). Precision measurement of half-lives and specific activities of U 235 and U 238. *Physical Review C*, *4*(5), 1889–1906. https://doi.org/10.1103/physrevc.4.1889

Khan, N. S., Ashe, E., Horton, B. P., Dutton, A., Kopp, R. E., Brocard, G., et al. (2017). Drivers of Holocene sea-level change in the Caribbean. *Quaternary Science Reviews*, *155*, 13–36. https://doi.org/10.1016/j.quascirev.2016.08.032

King, G. C., Stein, R. S., & Rundle, J. B. (1988). The growth of geological structures by repeated earthquakes 1. conceptual framework. *Journal of Geophysical Research*, *93*(B11), 13307–13318. https://doi.org/10.1029/jb093ib11p13307

Koba, M., Nakata, T., & Takahashi, T. (1982). Late Holocene eustatic sea-level changes deduced from geomorphological features and their ^{14}C dates in the Ryukyu Islands, Japan. *Palaeogeography, Palaeoclimatology, Palaeoecology*, *39*(3–4), 231–260. https://doi.org/10.1016/0031-0182(82)90024-4

Konishi, K., Schlanger, S. O., & Omura, A. (1970). Neotectonic rates in the central Ryukyu Islands derived from ^{230}Th coral ages. *Marine Geology*, *9*(4), 225–240. https://doi.org/10.1016/0025-3227(70)90049-6

Kopp, H., Weinzierl, W., Becel, A., Charvis, P., Evain, M., Flueh, E. R., et al. (2011). Deep structure of the central Lesser Antilles Island Arc: Relevance for the formation of continental crust. *Earth and Planetary Science Letters*, *304*(1–2), 121–134. https://doi.org/10.1016/j.epsl.2011.01.024

Kopp, R. E., Simons, F. J., Mitrovica, J. X., Maloof, A. C., & Oppenheimer, M. (2009). Probabilistic assessment of sea level during the Last Interglacial stage. *Nature*, *462*(7275), 863–867. https://doi.org/10.1038/nature08686

Kopp, R. E., Simons, F. J., Mitrovica, J. X., Maloof, A. C., & Oppenheimer, M. (2013). A probabilistic assessment of sea level variations within the Last Interglacial stage. *Geophysical Journal International*, *193*(2), 711–716. https://doi.org/10.1093/gji/ggt029

Laigle, M., Hirn, A., Sapin, M., Bécel, A., Charvis, P., Flueh, E., et al. (2013). Seismic structure and activity of the north-central Lesser Antilles subduction zone from an integrated approach: Similarities with the Tohoku forearc. *Tectonophysics*, *603*, 1–20. https://doi.org/10.1016/j.tecto.2013.05.043

Lambeck, K., & Chappell, J. (2001). Sea level change through the Last Glacial cycle. *Science*, *292*(5517), 679–686. https://doi.org/10.1126/science.1059549

Lardeaux, J.-M., Münch, P., Corsini, M., Cornée, J.-J., Verati, C., Lebrun, J.-F., et al. (2013). La Désirade island (Guadeloupe, French West Indies): A key target for deciphering the role of reactivated tectonic structures in Lesser Antilles arc building. *Bulletin de la Societe Geologique de France*, *184*(1–2), 21–34. https://doi.org/10.2113/gssgfbull.184.1-2.21

Leclerc, F. (2014). *Déformation active permanente induite par le mégachevauchement dans l'arc antillais: Apport des complexes récifaux quaternaires*. Institut de Physique du Globe de Paris.

Leclerc, F., & Feuillet, N. (2019). Quaternary coral reef complexes as powerful markers of long-term subsidence related to deep processes at subduction zones: Insights from Les Saintes (Guadeloupe, French West Indies). *Geosphere*, *15*(4), 983–1007. https://doi.org/10.1130/ges02069.1

Leclerc, F., Feuillet, N., Cabioch, G., Deplus, C., Lebrun, J., Bazin, S., et al. (2014). The Holocene drowned reef of Les Saintes plateau as witness of a long-term tectonic subsidence along the Lesser Antilles volcanic arc in Guadeloupe. *Marine Geology*, *355*, 115–135. https://doi.org/10.1016/j.margeo.2014.05.017

Leclerc, F., Feuillet, N., Perret, M., Cabioch, G., Bazin, S., Lebrun, J.-F., & Saurel, J. (2015). The reef platform of Martinique: Interplay between eustasy, tectonic subsidence and volcanism since Late Pleistocene. *Marine Geology*, *369*, 34–51. https://doi.org/10.1016/j.margeo.2015.08.001

Legendre, L., Philippon, M., Münch, P., Leticee, J.-L., Noury, M., Maincent, G., et al. (2018). Trench bending initiation: Upper plate strain pattern and volcanism. insights from the Lesser Antilles arc, St. Barthelemy island, French West Indies. *Tectonics*, *37*(9), 2777–2797. https://doi.org/10.1029/2017tc004921

Léticée, J.-L., Cornée, J.-J., Münch, P., Fietzke, J., Philippon, M., Lebrun, J.-F., et al. (2019). Decreasing uplift rates and Pleistocene marine terraces settlement in the central Lesser Antilles fore-arc (La Désirade Island, 16°N). *Quaternary International*, *508*, 43–59. https://doi.org/10.1016/j.quaint.2018.10.030

Lorscheid, T., Felis, T., Stocchi, P., Obert, J. C., Scholz, D., & Rovere, A. (2017). Tides in the Last Interglacial: Insights from notch geometry and palaeo tidal models in Bonaire, Netherland Antilles. *Scientific Reports*, *7*(1), 1–9. https://doi.org/10.1038/s41598-017-16285-6

Macharé, J., & Ortlieb, L. (1992). Plio-Quaternary vertical motions and the subduction of the Nazca Ridge, central coast of Peru. *Tectonophysics*, *205*(1–3), 97–108. https://doi.org/10.1016/0040-1951(92)90420-b

Manaker, D. M., Calais, E., Freed, A. M., Ali, S., Przybylski, P., Mattioli, G., et al. (2008). Interseismic plate coupling and strain partitioning in the northeastern Caribbean. *Geophysical Journal International*, *174*(3), 889–903. https://doi.org/10.1111/j.1365-246x.2008.03819.x

Martin-Kaye, P. H. A. (1959). *Reports on the geology of the leeward and British Virgin Islands*. Voice Publishing Company.

McCaffrey, R. (2008). Global frequency of magnitude 9 earthquakes. *Geology*, *36*(3), 263–266. https://doi.org/10.1130/g24402a.1

McCann, W. R., & Sykes, L. R. (1984). Subduction of aseismic ridges beneath the Caribbean plate: Implications for the tectonics and seismic potential of the northeastern Caribbean. *Journal of Geophysical Research*, *89*(B6), 4493–4519. https://doi.org/10.1029/jb089ib06p04493

Melnick, D. (2016). Rise of the central Andean coast by earthquakes straddling the Moho. *Nature Geoscience*, *9*(5), 401–407. https://doi.org/10.1038/ngeo2683

Meltzner, A. J., Sieh, K., Chiang, H.-W., Wu, C.-C., Tsang, L. L., Shen, C.-C., et al. (2015). Time-varying interseismic strain rates and similar seismic ruptures on the Nias–Simeulue patch of the Sunda megathrust. *Quaternary Science Reviews*, *122*, 258–281. https://doi.org/10.1016/j.quascirev.2015.06.003

Meyssignac, B., & Cazenave, A. (2012). Sea level: A review of present-day and recent-past changes and variability. *Journal of Geodynamics*, *58*, 96–109. https://doi.org/10.1016/j.jog.2012.03.005

Milne, G. A., & Mitrovica, J. X. (2008). Searching for eustasy in deglacial sea-level histories. *Quaternary Science Reviews*, *27*(25–26), 2292–2302. https://doi.org/10.1016/j.quascirev.2008.08.018

Mitrovica, J., Beaumont, C., & Jarvis, G. (1989). Tilting of continental interiors by the dynamical effects of subduction. *Tectonics*, *8*(5), 1079–1094. https://doi.org/10.1029/tc008i005p01079

Mitrovica, J., & Milne, G. (2002). On the origin of late Holocene sea-level highstands within equatorial ocean basins. *Quaternary Science Reviews*, *21*(20–22), 2179–2190. https://doi.org/10.1016/s0277-3791(02)00080-x

Muhs, D. R., Budahn, J. R., Prospero, J. M., & Carey, S. N. (2007). Geochemical evidence for African dust inputs to soils of western Atlantic islands: Barbados, the Bahamas, and Florida. *Journal of Geophysical Research*, *112*(F2), F02009. https://doi.org/10.1029/2005jf000445

Muhs, D. R., Simmons, K. R., Schumann, R. R., & Halley, R. B. (2011). Sea-level history of the past two interglacial periods: New evidence from U-series dating of reef corals from south Florida. *Quaternary Science Reviews*, *30*(5–6), 570–590. https://doi.org/10.1016/j.quascirev.2010.12.019

Muhs, D. R., Simmons, K. R., Schumann, R. R., Schweig, E. S., & Rowe, M. P. (2020). Testing glacial isostatic adjustment models of last-interglacial sea level history in the Bahamas and Bermuda. *Quaternary Science Reviews*, *233*, 106212. https://doi.org/10.1016/j.quascirev.2020.106212

Multer, H. G., Weiss, M. P., & Nicholson, D. V. (1986). *Antigua: Reefs, rocks & highroads of history (No. 1)*. Leeward Islands Science Associates.

O Leary, M. J., Hearty, P. J., Thompson, W. G., Raymo, M. E., Mitrovica, J. X., & Webster, J. M. (2013). Ice sheet collapse following a prolonged period of stable sea level during the Last Interglacial. *Nature Geoscience*, *6*(9), 796–800. https://doi.org/10.1038/ngeo1890

Opdyke, N., Spangler, D., Smith, D., Jones, D., & Lindquist, R. (1984). Origin of the epeirogenic uplift of Pliocene-Pleistocene beach ridges in Florida and development of the Florida karst. *Geology*, *12*(4), 226–228. https://doi.org/10.1130/0091-7613(1984)12<226:ooteuo>2.0.co;2

Paulatto, M., Laigle, M., Galve, A., Charvis, P., Sapin, M., Bayrakci, G., et al. (2017). Dehydration of subducting slow-spread oceanic lithosphere in the Lesser Antilles. *Nature Communications*, *8*(1), 1–11. https://doi.org/10.1038/ncomms15980

Paulay, G., & McEdward, L. R. (1990). A simulation model of island reef morphology: The effects of sea level fluctuations, growth, subsidence and erosion. *Coral Reefs*, *9*(2), 51–62. https://doi.org/10.1007/bf00368800

Philibosian, B., Feuillet, N., Weil-Accardo, J., Jacques, E., Guihou, A., Mériaux, A.-S., et al. (2022). 20th-century strain accumulation on the Lesser Antilles megathrust based on coral microatolls. *Earth and Planetary Science Letters*, *579*, 117343. https://doi.org/10.1016/j.epsl.2021.117343

Philibosian, B., Sieh, K., Avouac, J.-P., Natawidjaja, D. H., Chiang, H.-W., Wu, C.-C., et al. (2014). Rupture and variable coupling behavior of the Mentawai segment of the Sunda megathrust during the supercycle culmination of 1797 to 1833. *Journal of Geophysical Research: Solid Earth*, *119*(9), 7258–7287. https://doi.org/10.1002/2014jb011200

Pirazzoli, P. A., & Koba, M. (1989). Late Holocene sea-level changes in Iheya and Noho Islands, the Ryukyus, Japan. *Earth Science*, *43*(1), 1–6.

Polyak, V. J., Onac, B. P., Fornós, J. J., Hay, C., Asmerom, Y., Dorale, J. A., et al. (2018). A highly resolved record of relative sea level in the western Mediterranean Sea during the Last Interglacial period. *Nature Geoscience*, *11*(11), 860–864. https://doi.org/10.1038/s41561-018-0222-5

Robson, G. (1964). An earthquake catalogue for the Eastern Caribbean 1530-1960. *Bulletin of the Seismological Society of America*, *54*(2), 785–832. https://doi.org/10.1785/bssa0540020785

Rohling, E. J., Hibbert, F. D., Grant, K. M., Galaasen, E. V., Irvalı, N., Kleiven, H. F., et al. (2019). Asynchronous Antarctic and Greenland ice-volume contributions to the Last Interglacial sea-level highstand. *Nature Communications*, *10*(1), 1–9. https://doi.org/10.1038/s41467-019-12874-3

Rovere, A., Raymo, M. E., Mitrovica, J., Hearty, P. J., O Leary, M., & Inglis, J. (2014). The Mid-Pliocene sea-level conundrum: Glacial isostasy, eustasy and dynamic topography. *Earth and Planetary Science Letters*, *387*, 27–33. https://doi.org/10.1016/j.epsl.2013.10.030

Rovere, A., Raymo, M. E., Vacchi, M., Lorscheid, T., Stocchi, P., Gomez-Pujol, L., et al. (2016). The analysis of Last Interglacial (MIS 5e) relative sea-level indicators: Reconstructing sea-level in a warmer world. *Earth-Science Reviews*, *159*, 404–427. https://doi.org/10.1016/j.earscirev.2016.06.006

Rowley, D. B., Forte, A. M., Moucha, R., Mitrovica, J. X., Simmons, N. A., & Grand, S. P. (2013). Dynamic topography change of the eastern United States since 3 million years ago. *Science*, *340*(6140), 1560–1563. https://doi.org/10.1126/science.1229180

Ruff, L., & Kanamori, H. (1980). Seismicity and the subduction process. *Physics of the Earth and Planetary Interiors*, *23*(3), 240–252. https://doi.org/10.1016/0031-9201(80)90117-x

Ruff, L., & Kanamori, H. (1983). Seismic coupling and uncoupling at subduction zones. *Tectonophysics*, *99*(2–4), 99–117. https://doi.org/10.1016/0040-1951(83)90097-5

Ruiz, M., Galve, A., Monfret, T., Sapin, M., Charvis, P., Laigle, M., et al. (2013). Seismic activity offshore Martinique and Dominica islands (Central Lesser Antilles subduction zone) from temporary onshore and offshore seismic networks. *Tectonophysics*, *603*, 68–78. https://doi.org/10.1016/j.tecto.2011.08.006

Russell, R. J., & McIntire, W. G. (1966). *Barbuda reconnaissance (Tech. Rep.)*. Louisiana State Univ Baton Rouge Coastal Studies Inst.

Saillard, M., Audin, L., Rousset, B., Avouac, J.-P., Chlieh, M., Hall, S. R., et al. (2017). From the seismic cycle to long-term deformation: Linking seismic coupling and Quaternary coastal geomorphology along the Andean megathrust. *Tectonics*, *36*(2), 241–256. https://doi.org/10.1002/2016tc004156

Savage, J. C. (1983). A dislocation model of strain accumulation and release at a subduction zone. *Journal of Geophysical Research*, *88*(B6), 4984–4996. https://doi.org/10.1029/jb088ib06p04984

Schaeffer, A., & Lebedev, S. (2013). Global shear speed structure of the upper mantle and transition zone. *Geophysical Journal International*, *194*(1), 417–449. https://doi.org/10.1093/gji/ggt095

Sepulcre, S., Durand, N., & Bard, E. (2009). Mineralogical determination of reef and periplatform carbonates: Calibration and implications for paleoceanography and radiochronology. *Global and Planetary Change*, *66*(1–2), 1–9. https://doi.org/10.1016/j.gloplacha.2008.07.008

Spencer, T. (1985). Weathering rates on a Caribbean reef limestone: Results and implications. *Marine Geology*, *69*(1–2), 195–201. https://doi.org/10.1016/0025-3227(85)90142-2

Stein, S., Engeln, J. F., Wiens, D. A., Fujita, K., & Speed, R. C. (1982). Subduction seismicity and tectonics in the Lesser Antilles arc. *Journal of Geophysical Research*, *87*(B10), 8642–8664. https://doi.org/10.1029/jb087ib10p08642

Symithe, S., Calais, E., De Chabalier, J., Robertson, R., & Higgins, M. (2015). Current block motions and strain accumulation on active faults in the Caribbean. *Journal of Geophysical Research: Solid Earth*, *120*(5), 3748–3774. https://doi.org/10.1002/2014jb011779

Taylor, F. W., Edwards, R. L., Wasserburg, G., & Frohlich, C. (1990). Seismic recurrence intervals and timing of aseismic subduction inferred from emerged corals and reefs of the central Vanuatu (New Hebrides) frontal arc. *Journal of Geophysical Research*, *95*(B1), 393–408. https://doi.org/10.1029/jb095ib01p00393

Taylor, F. W., Frohlich, C., Lecolle, J., & Strecker, M. (1987). Analysis of partially emerged corals and reef terraces in the central Vanuatu arc: Comparison of contemporary coseismic and nonseismic with Quaternary vertical movements. *Journal of Geophysical Research*, *92*(B6), 4905–4933. https://doi.org/10.1029/jb092ib06p04905

Taylor, F. W., Isacks, B., Jouannic, C., Bloom, A., & Dubois, J. (1980). Coseismic and Quaternary vertical tectonic movements, Santo and Malekula Islands, New Hebrides island arc. *Journal of Geophysical Research*, *85*(B10), 5367–5381. https://doi.org/10.1029/jb085ib10p05367

Thirumalai, K., Taylor, F. W., Shen, C.-C., Lavier, L. L., Frohlich, C., Wallace, L. M., et al. (2015). Variable Holocene deformation above a shallow subduction zone extremely close to the trench. *Nature Communications*, *6*(1), 1–6. https://doi.org/10.1038/ncomms8607

Thompson, W. G., & Goldstein, S. L. (2005). Open-system coral ages reveal persistent suborbital sea-level cycles. *Science*, *308*(5720), 401–404. https://doi.org/10.1126/science.1104035

Toomey, M., Ashton, A. D., & Perron, J. T. (2013). Profiles of ocean island coral reefs controlled by sea-level history and carbonate accumulation rates. *Geology*, *41*(7), 731–734. https://doi.org/10.1130/g34109.1

Trenhaile, A. S. (2015). Coastal notches: Their morphology, formation, and function. *Earth-Science Reviews*, *150*, 285–304. https://doi.org/10.1016/j.earscirev.2015.08.003

Trudgill, S. (1979). Surface lowering and landform evolution on Aldabra. *Philosophical Transactions of the Royal Society of London B Biological Sciences*, *286*(1011), 35–45.

van Rijsingen, E., Calais, E., Jolivet, R., de Chabalier, J. B., Jara, J., Symithe, S., et al. (2020). *Inferring interseismic coupling along the lesser Antilles arc: A Bayesian approach*.

Vermeesch, P. (2018). IsoplotR: A free and open toolbox for geochronology. *Geoscience Frontiers*, *9*(5), 1479–1493. https://doi.org/10.1016/j.gsf.2018.04.001

Veron, J. E. N. (1995). *Corals in space and time: The biogeography and evolution of the Scleractinia*. Cornell University Press.

Viles, H., & Trudgill, S. (1984). Long term remeasurements of micro-erosion meter rates, Aldabra Atoll, Indian Ocean. *Earth Surface Processes and Landforms*, *9*(1), 89–94. https://doi.org/10.1002/esp.3290090111

Waelbroeck, C., Labeyrie, L., Michel, E., Duplessy, J. C., McManus, J., Lambeck, K., et al. (2002). Sea-level and deep water temperature changes derived from benthic foraminifera isotopic records. *Quaternary Science Reviews*, *21*(1–3), 295–305. https://doi.org/10.1016/s0277-3791(01)00101-9

Wang, Y., Shyu, J. B. H., Sieh, K., Chiang, H.-W., Wang, C.-C., Aung, T., et al. (2013). Permanent upper plate deformation in Western Myanmar during the great 1762 earthquake: Implications for neotectonic behavior of the northern Sunda megathrust. *Journal of Geophysical Research: Solid Earth*, *118*(3), 1277–1303. https://doi.org/10.1002/jgrb.50121

Watters, D. R., Donahue, J., & Stuckenrath, R. (1992). Paleoshorelines and the prehistory of Barbuda, West Indies. In *Paleoshorelines and prehistory: An investigation of method* (pp. 15–52).

Webster, J., Davies, P., & Konishi, K. (1998). Model of fringing reef development in response to progressive sea level fall over the last 7000 years–(Kikai-jima, Ryukyu Islands, Japan). *Coral Reefs*, *17*(3), 289–308. https://doi.org/10.1007/s003380050131

Weil-Accardo, J., Feuillet, N., Jacques, E., Deschamps, P., Beauducel, F., Cabioch, G., et al. (2016). Coral microatolls of Martinique (French West Indies) record 230 years of relative sea-level changes due to climate and megathrust tectonics. *Journal of Geophysical Research: Solid Earth*.

Weil-Accardo, J., Feuillet, N., Satake, K., Goto, T., Goto, K., Harada, T., et al. (2020). Relative sea-level changes over the past centuries in the central Ryukyu Arc inferred from coral microatolls. *Journal of Geophysical Research: Solid Earth*, *125*(2), e2019JB018466. https://doi.org/10.1029/2019jb018466

Wesson, R. L., Melnick, D., Cisternas, M., Moreno, M., & Ely, L. L. (2015). Vertical deformation through a complete seismic cycle at Isla Santa Maria, Chile. *Nature Geoscience*, *8*(7), 547–551. https://doi.org/10.1038/ngeo2468

Westbrook, G., Ladd, J., Buhl, P., Bangs, N., & Tiley, G. (1988). Cross section of an accretionary wedge: Barbados Ridge complex. *Geology*, *16*(7), 631–635. https://doi.org/10.1130/0091-7613(1988)016<0631:csoaaw>2.3.co;2

Wigley, P. (1977). Facies analysis of Holocene carbonate sediments and tertiary (?)-Pleistocene limestones on and around Barbuda, West Indies: Sediments and diagenesis. *Studies in Geology*, *4*.